

1 **Analog~~ue~~e experiments on releasing and restraining bends and their**
2 **application to the study of the Barents Shear Margin**

3
4
5
6 **Roy H. Gabrielsen¹⁾, Panagiotis A. Giannenas²⁾, Dimitrios Sokoutis^{1,3)}, Ernst**
7 **Willingshofer³⁾, Muhammad Hassaan^{1,4)} & Jan Inge Faleide¹⁾**

8
9 ¹⁾ Department of Geosciences, University of Oslo, Norway

10 ²⁾ Univ Rennes, CNRS, Géosciences Rennes, UMR 6118, 35000 Rennes, France

11 ³⁾ Faculty of Geosciences, Utrecht University, the Netherlands

12 ⁴⁾ Vår Energi AS, Grundingen 3, 0250 Oslo, Norway

13
14
15 **Corresponding author: Roy H. Gabrielsen (r.h.gabrielsen@geo.uio.no)**

16
17 **ORCI-id:**

18 Jan Inge Faleide: 0000-0001-8032-2015

19 Roy H. Gabrielsen: 0000-0001-5427-8404

20 Muhammad Hassaan: 0000-0001-6004-8557

21
22
23
24
25 **Abstract:**

26 The Barents Shear Margin separates the Svalbard and Barents Sea from the
27 North Atlantic. During the break-up of the North Atlantic the plate tectonic
28 configuration was characteri~~s~~zed by sequential dextral shear, extension, and
29 eventually contraction and inversion. This generated a complex zone of
30 deformation that contains several structural families of over-lapping and
31 reactivated structures.

32 A series of crustal-scale analogue experiments, utili~~s~~zing a scaled stratified sand-
33 silicon polymer sequence were utili~~s~~zed in the study of the structural evolution
34 of the shear margin.

35
36 The most significant observations for interpreting the structural configuration of
37 the Barents Shear Margin are:

38 1) Prominent early-stage positive structural elements (e.g. folds, push-ups)
39 interacted with younger (e.g. inversion) structures and contributed to a hybrid
40 final structural pattern.

41 2) Several structural features that were initiated during the early (dextral shear)
42 stage became overprinted and obliterated in the subsequent stages.

43 3) All master faults, pull-part basins and extensional shear duplexes initiated
44 during the shear stage quickly became linked in the extension stage, generating a
45 connected basin system along the entire shear margin at the stage of maximum
46 extension.

47 4) The fold pattern generated during the terminal stage (contraction/inversion)
48 became dominant in the basin areas and was characteri~~s~~zed by fold axes striking
49 parallel to the basin margins. These folds, however, strongly affected the shallow
50 intra-basin layers.

51 The experiments reproduced the geometry and positions of the major basins and
52 relations between structural elements (fault and fold systems) as observed along
53 and adjacent to the Barents Shear Margin. This supports the present structural
54 model for the shear margin.

55
56

57 **Plain language summary:**

58 The Barents Shear Margin defines the border between the relatively shallow
59 Barents Sea that is situated on a continental plate, and the deep ocean. The
60 margin is characterized by a complex structural pattern that has resulted from
61 the opening and separation of the continent and the ocean, starting c. 65 million
62 years ago. This history included on phase of right-lateral shear and one phase of
63 spreading, the latter including a sub-phase of shortening, perhaps due to plate
64 tectonic reorganizations. The area has been mapped by the study of reflection
65 seismic lines for decades, but many details of its development is not yet fully
66 constrained. We therefore ran a set of scaled experiments to investigate what
67 kind of structures could be expected in ~~this kind of~~ tectonic environment, and to
68 figure out what is a reasonable time relation between them. From these
69 experiments we deducted several types of structures (faults, folds and
70 sedimentary basins) that help us to improve the understanding of the history of
71 the opening of the North Atlantic.

72
73
74

75 **Key words:** Analogue experiments, dextral strike-slip, releasing and restraining
76 bends, multiple folding, Barents Shear Margin, basin inversion

77
78

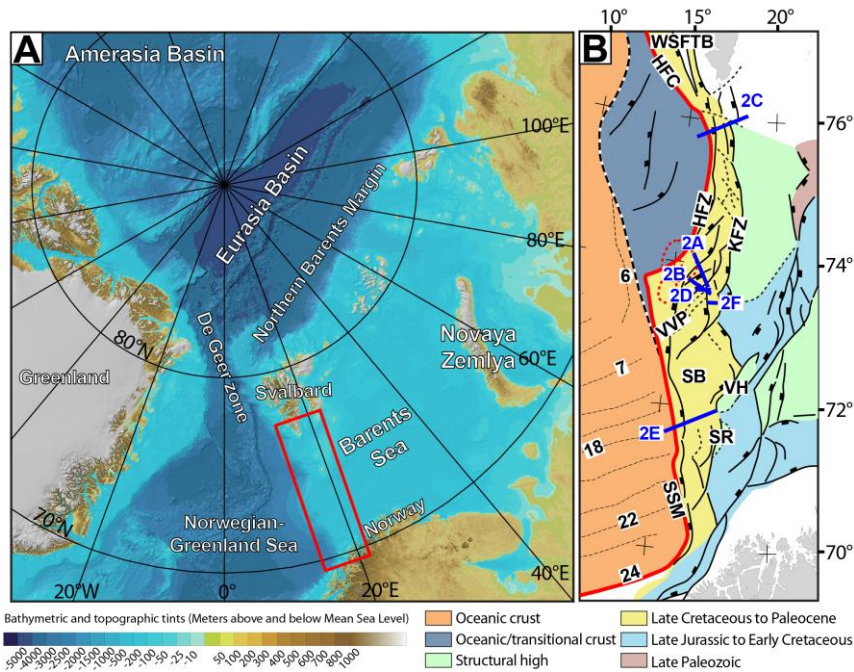
79 **Introduction**

80
81 Physiography, width and structural style of the Norwegian continental margin
82 vary considerably along its strike (e.g. Faleide et al., 2008, 2015). The margin
83 includes a southern rifted segment between 60° and 70°N and a northern
84 sheared-rifted segment between 70° and 82°N (**Figure 1A**). The latter coincides
85 with the ocean-ward border of the western Barents Sea and Svalbard margins
86 (e.g. Faleide et al., 2008) and is referred to here as “the Barents Shear Margin”.
87 This segment coincides with the continent-ocean transition (COT) of the
88 northernmost part of the North Atlantic Ocean, ~~and its~~ configuration is typical
89 for that of transform margins where the structural pattern became established in
90 an early stage of shear, later to develop into an active continent-ocean passive
91 margin (Masclé & Blarez, 1987; Lorenzo, 1997; Seiler et al., 2010; Basile, 2015;
92 Nemcok et al., 2016).

93 Late Cretaceous - Palaeocene shear, rifting, breakup and incipient spreading in
94 the North Atlantic was associated with voluminous magmatic activity, resulting
95 in the development of the North Atlantic Volcanic Province (Saunders et al.,
96 1997; Ganerød et al., 2010; Horni, 2017). According to its tectonic development,
97 the Barents Shear Margin (**Figure 1B**) incorporates, or is bordered by, several
98 distinct structural elements, some of which are associated with volcanism and
99 halokinesis.

100 The multistage development combined with a complex geometry caused
101 interference between structures (and sediment systems) in different stages of
102 the margin development. Such relations are not always obvious, but
103 interpretation can be supported by the help of scale-models. We combine the
104 interpretation of reflection seismic data and analogue modeling. Thus, we
105 investigate structures generated in ~~(initial)~~ dextral shear. These were generated
106 during initial dextral shear the development into seafloor spreading and
107 subsequent contraction. The later stages (contraction) were likely influenced by
108 plate reorganization (Talwani & Eldholm, 1977; Gaina et al., 2009; see also
109 Vågnes et al., 1998; Pascal & Gabrielsen, 2001; Pascal et al., 2005; Gac et al.,
110 2016) or other far-field stresses (Doré & Lundin, 1996; Lundin & Doré, 1997;
111 Doré et al., 1999; 2016; Lundin et al., 2013). The present experiments were
112 designed to illuminate the structural complexity affiliated with multistage

113 sheared passive margins, so that the significance of structural elements like fault
 114 and fold systems observed along the Barents Shear Margin could be set into a
 115 dynamic context. The study area suffered



116
 117 **Figure 1: A)** The Barents Sea is separated from the Norwegian-Greenland Sea by
 118 the de Geer transfer margin. Red box shows the present study area. **B)** Structural
 119 map of the Barents Sea shear margin. Note segmentation of the continent-
 120 ocean transition. Abbreviations (from north to south): WSFTB = West
 121 Spitsbergen Fold-and-Thrust Belt, HFZ = Hornsund Fault Complex, KFC =
 122 Knølegga Fault Zone, VVP = Vestbakken Volcanic Province, SB = Sørvestsnaget
 123 Basin, VH = Veslemøy High, SR = Senja Ridge, SSM = Senja Shear Margin. Blue
 124 lines indicate position of seismic profiles in Figure 2 and red line X-X' shows
 125 western border of thinned crust (see also Figure 3). Chron numbers are
 126 indicated on oceanic crust area.
 127

128 repeated and contrasting stages of deformation, including dextral shear, oblique
 129 extension, inversion and volcanic activity. This is a particular challenge in such
 130 tectonic settings that are characterized by repeated overprinting and
 131 cannibalization of younger structural elements. Results from the experiments
 132 facilitate the identification and characterization of structural elements at the
 133 different stages of deformation. Additionally, they allow to identify the

134 structural elements that were developed at stages of deformation preceding the
135 present-day margin configuration.

136

137

138 **Regional background**

139 In the following sections we provide definitions and a short description of the
140 main structural elements constituting the study area. The structural elements
141 are presented in-sequence from north to south (**Figure 1B**).

142 The greater **Barents Shear Margin** is a part of the more extensive De
143 Geer Zone mega shear system which linked the Norwegian Greenland Sea and
144 the Arctic Eurasia system (Eldholm et al., 1987; 2002; Faleide et al., 1988;
145 Breivik et al., 1998; 2003). Together with its conjugate Greenland counterpart it
146 carries the evidence of post-Caledonian extension that culminated with Cenozoic
147 break-up of the North Atlantic (e.g. Brekke, 2000; Gabrielsen et al., 1990; Faleide
148 et al., 1993; Gudlaugsson et al., 1998). Two shear margin segments are separated
149 by a central rift-dominated segment along the Barents Shear Margin (Myhre et
150 al., 1982; Vågnes, 1997; Myhre & Eldholm, 1988; Ryseth et al., 2003; Faleide at
151 al., 1988; 1993; 2008). Each segment maintained the structural and magmatic
152 characteristics of the crust during its development. Of these the Senja Shear
153 Margin is the southernmost segment, originally termed the Senja Fracture Zone
154 by Eldholm et al. (1987). Here NNW-SSE-striking folds interfere with NE-SW-
155 striking structures (Giannenas, 2018). Strain partitioning characterizes the shear
156 zone system (e.g. West Spitsbergen; Leever et al., 2011a,b and the Sørvestsnaget
157 Basin; Kristensen et al., 2017).

158

159 **The Hornsund Fault Zone and West Spitsbergen Fold-and Thrust Belt** form
160 the northernmost segment of the Barents Shear Margin. It coincides with the
161 southern continuation of the De Geer Zone and the Senja Shear Margin. The
162 Hornsund Fault Zone belongs to this system and provides a type setting for
163 transpression and strain partitioning together with the West Spitsbergen fold-
164 and-thrust-belt (Harland, 1965; 1969; 1971; Lowell, 1972; Gabrielsen et al.,
165 1992; Maher et al., 1997; Leever et al., 2011 a,b). Plate tectonic reconstructions
166 suggest that the plate boundary accommodated c. 750 km along-strike dextral

167 displacement and 20-40 km of shortening in the Eocene (Bergh et al., 1997;
168 Gaina et al., 2009).

169

170 **The Knølegga Fault Zone** can be seen as a part of the Hornsund fault system
171 extending from the southern tip of Spitsbergen (Gabrielsen et al., 1990). It trends
172 NNE-SSW to N-S and defines the western margin of the Stappen High. The
173 vertical displacement approaches 6 km. Although the main movements along the
174 fault may be Tertiary of age, it is likely that it was initiated much earlier. The
175 Tertiary displacement may have a lateral (dextral) component (Gabrielsen et al.,
176 1990).

177

178 **The Vestbakken Volcanic Province** is the main topic of this contribution. It
179 represents the central rifted segment of the Barents Shear Margin and links the
180 sheared margin segments to the north and south occupying a right-double
181 stepping (eastward) releasing-bend-setting. Prominent volcanoes and sill-
182 intrusions suggest three distinct volcanic events in the Vestbakken Volcanic
183 Province (Jebsen & Faleide, 1998; Faleide et al., 2008; Libak et al., 2012). It is
184 constrained to its east by the eastern boundary fault (EBF in **Figure 1B**), that is a
185 part of the Knølegga Fault Complex, separating the Vestbakken Volcanic Province
186 from the marginal Stappen High to the east. To the south and southeast the
187 Vestbakken Volcanic Province drops gradually towards the Sørvestsnaget Basin
188 across the southern extension of the eastern boundary fault and its associated
189 faults. To the west and north the area is delineated by the continent - ocean
190 boundary/transition. The Vestbakken Volcanic Province includes both
191 extensional and contractional structures (e.g. Jebsen & Faleide, 1998; Faleide et
192 al., 2008; Blaich et al., 2017). Two main episodes of Cenozoic extensional faulting
193 were identified in the Vestbakken Volcanic Province: (i) a late Paleocene-early
194 Eocene event, which correlates in time with the continental break-up in the
195 Norwegian-Greenland Sea, (ii) an early Oligocene event that is tentatively
196 correlated to plate reorganization around 34 Ma activating NE-SW striking faults.
197 Volcanic activity coincides with these events.

198

199 **The Sørvestsnaget Basin** occupies the area east ~~of~~ the COT between 71 and
200 73°N and is characteri~~s~~zed by an exceptionally thick Cretaceous-Cenozoic
201 sequence (Gabrielsen et al., 1990). To the west it is delineated by the Senja Shear
202 Margin and to the northeast it is separated from the Bjørnøya Basin by the
203 southern part of the Knølegga Fault Complex (Faleide et al., 1988). The position
204 of the Senja Ridge coincides with southeastern border of the Sørvestsnaget Basin
205 (**Figure 1B**), whereas the Vestbakken Volcanic Province is situated to its north.
206 An episode of Cretaceous rifting in the Sørvestsnaget Basin climaxed in the
207 Cenomanian-middle Turonian (Breivik et al., 1998), succeeded by Late
208 Cretaceous-Palaeocene fast sedimentation (Ryseth et al., 2003). Particularly the
209 later stages of the basin formation were strongly influenced by the opening of
210 the North Atlantic (Hanisch, 1984; Brekke & Riis, 1987). Salt diapirism also
211 contributed to the development of this basin (Perez-Garcia et al., 2013).

212

213 **The Senja Ridge** (SR in **Figure 1B**) runs parallel to the continental margin and
214 coincides with the western border of the Tromsø Basin. It is characteri~~s~~zed by a
215 N-S-trending gravity anomaly which ~~isare~~ interpreted as buried mafic-ultramafic
216 intrusions which are associated with the Seiland Igneous Province (Fichler &
217 Pastore, 2022). The structural development of the Senja Ridge has been
218 associated with shear affiliated with the development of the shear margin (Riis
219 et al., 1986) and though it ~~documented that it~~ was a positive structural element
220 from the mid Cretaceous to the Pliocene it may have been activated at an even
221 earlier stage (Gabrielsen et al., 1990).

222

223 **The Senja Shear Margin** was active during the Eocene opening of the
224 Norwegian-Greenland Sea dextral shear causing splitting ~~offout~~ of slivers of
225 continental crust. These slivers became embedded in the oceanic crust during
226 continued seafloor spreading (Faleide et al., 2008). The Senja Shear Margin
227 coincides with the western margin of a basin system superimposed on an area of
228 significant crustal thinning. This part of the shear margin was characteri~~s~~zed by
229 a composite architecture even ~~duringat~~ the earliest stages of its development
230 (Faleide et al., 2008). The basin system accumulated sedimentary sequences that
231 reached thicknesses of up to 18-20 km. Subsequent shearing contributed to the

Formatted: Font: Bold, Not Highlight

232 development of releasing and restraining bends, associated pull-apart-basins,
233 neutral strike-slip segments, flower-structures and fold-systems (*sensu* Crowell,
234 1974 a,b; Biddle & Christie-Blick, 1985a,b; Cunningham & Mann, 2007a,b).
235 Particularly the hanging wall west of the Knølegga Fault Complex (see below) of
236 the Barents Shear Margin was affected by wrench deformation as seen from
237 several push-ups and fold systems (Grogan et al., 1999; Bergh & Grogan 2003).
238 The structural development of the margin was complicated by active halokinesis
239 (Knutsen & Larsen, 1997; Gudlaugsson et al., 1998; Ryseth et al., 2003).

240

241 **Reflection seismic data and structural interpretation**

242 The data set of this study includes 2D seismic reflection data from several surveys
243 and well data in the Vestbakken Volcanic Province. Data coverage is less dense in the
244 northern part of the study area. Typical spacing of seismic lines is 4 km. Well 7316/5-
245 1 was used to correlate the seismic data with formation tops in the study area
246 ~~while~~ previously published ~~paper-based~~ correlations provided calibration and
247 age of each seismic horizon ~~mapped~~ (e.g. Eidvin et al., 1993; 1998 Ryseth et al.,
248 2003). Three stratigraphic groups are encountered in the well, namely ~~the~~ Nordland
249 Group (between 473 - 945 m); the Sotbakken Group (between 945-3752m) and
250 Nygrunnen Group (between 3752-4014m) (Eidvin et al., 1993; 1998;
251 www.npd.noceom). Several folds of regional significance and with axial traces that
252 can be followed along strike for 2-3 km or more occur in the Vestbakken Volcanic
253 Province. The folds are commonly ~~are~~ situated in the hanging walls of extensional
254 faults and the fold traces and the structural grain of the thick-skinned master faults are
255 generally parallel. This shows that the position and orientation of the folds were
256 determined by the preexisting basement structural fabric. The mapping of the folds is
257 constrained by the spacing of reflection seismic lines, so each fold trace may include
258 undetected overlap-zones or axial off-sets. The folds were identified on the lower
259 Eocene, Oligocene and lower Miocene levels. All the mapped folds are either
260 positioned in the hanging walls of extensional (sometimes inverted) master faults or
261 are dissected by younger faults with minor throws.

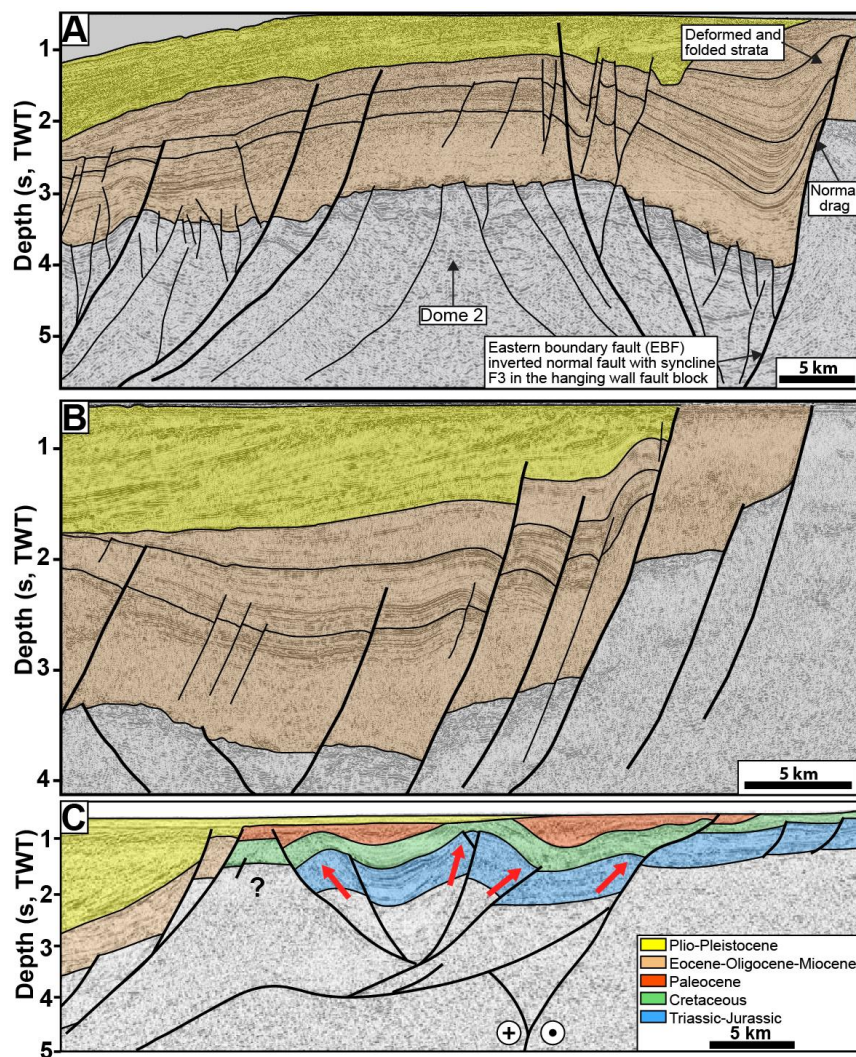
262

263 **Strike-slip systems and analogue shear experiments**

Formatted: Default Paragraph Font, Font: (Default)
+Body (Cambria), Not Highlight

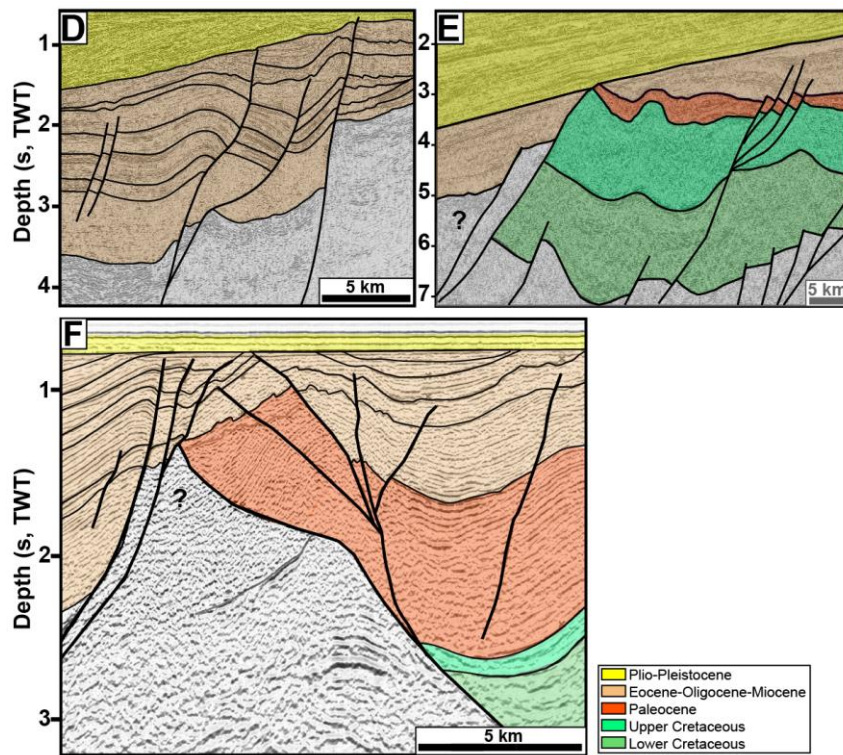
Formatted: Default Paragraph Font, Font: (Default)
+Body (Cambria), Not Highlight

264 Shear margins and strike-slip systems are structurally complex and highly
 265 dynamic, so that the ultimate eventual architecture of such systems
 266 contains include structural elements that were not contemporaneous (e.g.
 267 Graymer et al., 2007; Crowell, 1962; 1974a,b; Woodcock & Fischer, 1986;
 268 Mousloupoulou et al., 2007; 2008). Analogue models offer the option to study the
 269 dynamics of such relations and therefore attracted the attention of early workers
 270 in this field (e.g. Cloos, 1928; Riedel, 1929) and have continued to do so until
 271 today. Early experimental works



272

273
274
275
276
277
278
279
280



281

282 **Figure 2:** Seismic examples, Vestbakken Volcanic Province. **A)** Gentle, partly
283 collapsed NE-SW-striking anticline/dome of uncertain origin in the eastern
284 terrace domain of the southern Vestbakken Volcanic Province. **B,C)**
285 Asymmetrical folds (fold family 2; Giannenas 2018) situated along the eastern
286 margin of the Vestbakken Volcanic Province. These may represent primary SPE-
287 4-structures focused in the hanging walls along margins of master fault blocks,
288 representing reactivated SPE-2-structures. **D)** trains of symmetrical folds with
289 upright fold axes (corresponding to PSE-5-structures) are preserved inside
290 larger fault blocks. See text for explanation of SPE-structures. **E)** Section through

291 push-up associated with restraining bend (PSE-4-structure). **F**) Flower (PSE-2)-
292 structure in aera dominated by neutral shear.

293

294 mostly utilized one-layer (“Riedel-box”) models (e.g. Emmons, 1969; Tchalenko,
295 1970; Wilcox et al., 1973), which were soon to be expanded by the study of
296 multilayer systems (e.g. Faugère et al., 1986; Naylor et al., 1986; Richard et al.,
297 1991; Richard & Cobbold, 1989, 1995; Schreurs, 1994, 2003; Manduit & Dauteuil,
298 1996; Dateuil & Mart, 1998; Schreurs & Colletta, 1998, 2003; Ueta et al., 2000;
299 Dooley & Schreurs, 2012). The systematics and dynamics of strike-slip systems
300 have been focused upon in a number of summaries like Sylvester (1985; 1988);
301 Biddle & Christie-Blick (1985 a,b); Cunningham & Mann (2007); Dooley &
302 Schreurs (2012); Nemcok et al. (2016) and Peacock et al. (2016). Concepts and
303 nomenclature established in these works are used in the following descriptions
304 and analysis. Also, following Christie-Blick & Biddle (1985a,b) and Dooley &
305 Schreurs (2012) we apply the term Principal Deformation Zone (PDZ) for the
306 junction between the movable polythene plates underlying the experiment. The
307 contact between the fixed and movable base defined a non-stationary velocity
308 discontinuity (“VD”; Ballard et al., 1987; Allemand & Brun, 1991; Tron & Brun,
309 1991).

310 Several experimental works have particularly focused on the geometry
311 and development of pull-apart-basins in releasing bend settings (Mann et al.,
312 1983; Faugère et al., 1983; Richard et al., 1995; Dooley & McClay, 1997; Basile &
313 Brun, 1999; Sims et al., 1999; Le Calvez & Vendeville, 2002; Mann, 2007; Mitra &
314 Paul, 2011). The pull-apart basin was described by Burchfiel & Stewart (1966)
315 and Crowell (1974a,b) as formed at a releasing bend or at a releasing fault step-
316 over along a strike-slip zone (Biddle & Christie-Blick, 1985a,b). This basin type
317 has also been termed “rhomb grabens” (Freund, 1971) and “strike-slip basins”
318 (Mann et al., 1993) and is commonly considered to be synonymous with the
319 extensional strike-slip duplex (Woodcock & Fischer, 1986; Dooley & Schreurs,
320 2012). In the descriptions of our experiments, we found it convenient to
321 distinguish between extensional strike-slip duplexes in the context of Woodcock
322 & Fischer (1986) and Twiss & Moores (2007, p. 140-141) and pull-apart basins
323 (rhomb grabens: Crowell, 1974 a,b; Aydin & Nur, 1993) since they reflect slightly
324 different stages in the development in our experiments (see discussion).

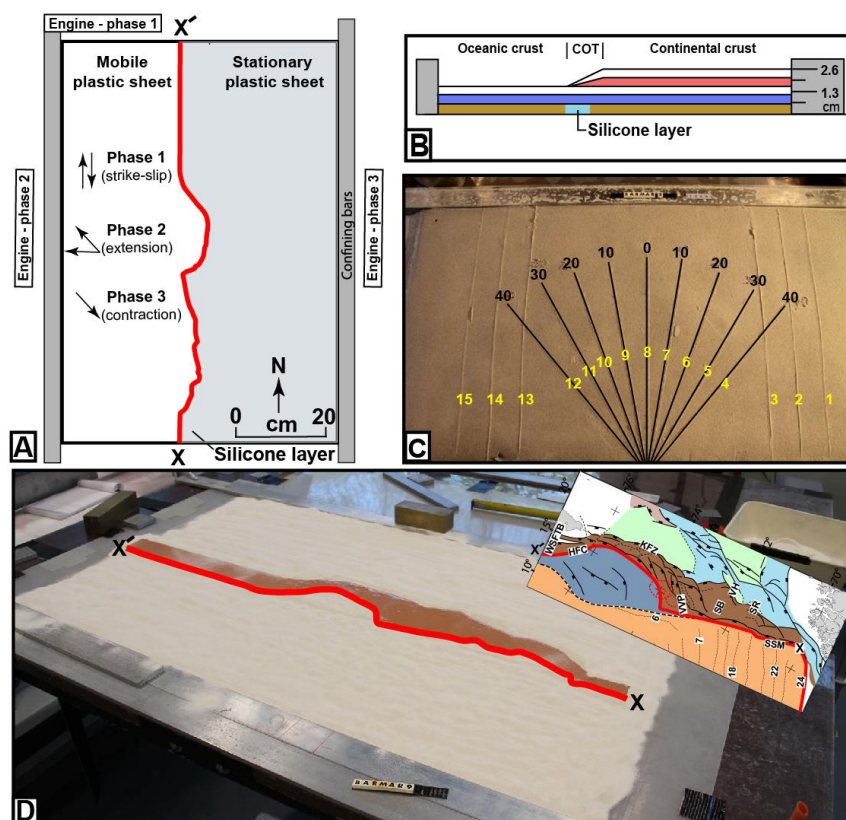
325

326 **Experimental setup**

327 To study the kinematics of complex shear margins, a series of analogue
328 experiments were performed at the tectonic modelling laboratory (TecLab) of
329 Utrecht University, The Netherlands. All experiments were built on two
330 overlapping 1 mm thick plastic sheets (each 100 cm long and 50 cm wide) that
331 were placed on a flat, horizontal table surface. The boundary between the
332 underlying movable and overlying stationary plastic sheets had the shape of the
333 mapped continent-ocean boundary (COB; **Figure 1B**). The moveable sheet was
334 connected to an electronic engine, which pulled the sheet at constant velocity
335 during all three deformation stages. Displacement rates were therefore not
336 scaled. The modelling material was then placed on these sheets where the layers
337 on the stationary sheet represent the continental crust including the continent-
338 ocean transition (COT) whereas those on the mobile sheet represents the
339 oceanic crust. The model layers were confined by aluminum bars along the long
340 sides and sand along the short sides (**Figure 3A**). The continental crust tapers off
341 towards the oceanic crust with a relatively constant gradient. A sand-wedge with
342 a constant dip angle determined by the difference in thickness between the
343 intact and the stretched crust, and that covered the width of the silicon putty
344 layer, was made to simulate the ocean-continent transition (**Figure 3B**). The
345 taper angle was kept constant for all models.

346 The pre-cut shape of the plate boundary includes major releasing bends
347 positioned so that they correspond to the geometry of the COB and the three
348 main structural segments of the Barents Shear Margin as follows. *Segment 1* of
349 the BarMar-experiments (**Figure 4**) contained several sub-segments with
350 releasing and restraining bends as well as segments of “neutral” (Wilcox et al.,
351 1973; Mann et al. 1983; Biddle & Christie-Blick, 1985b) or “pure” (Richard et al.,
352 1991) strike-slip. *Segment 2* had a basic crescent shape, thereby defining a
353 releasing bend at its southern margin in the position similar to that of the
354 Vestbakken Volcanic Province that merged into a neutral shear-segment along
355 the strike of, whereas a restraining bend occupied the northern margin of the
356 segment. *Segment 3* was a straight basement segment, defining a zone of neutral
357 shear and corresponds to the strike-slip segment west of Svalbard (**Figure 1**).

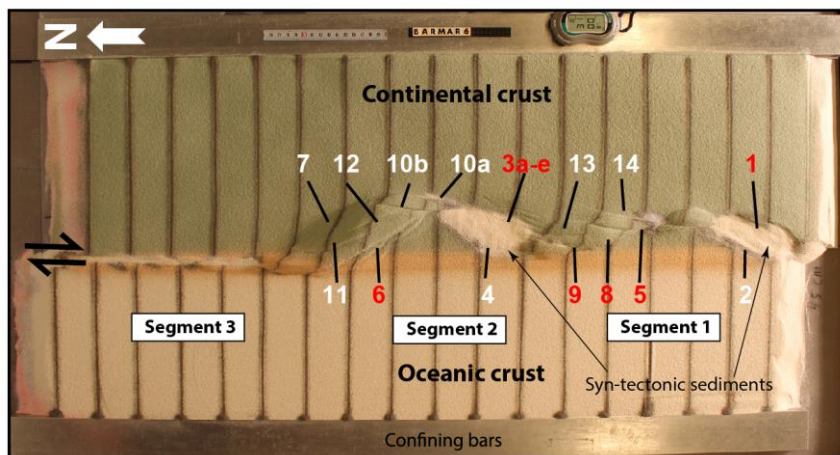
358 The experiments included three stages of deformation with constant rates
 359 of movement of the mobile sheet at 10 cmhr^{-1} in all three stages. The relative
 360 angles of plate movements in the experiments were taken from post late
 361 Paleocene opening directions in the northeast Atlantic (Gaina et al., 2009).
 362 Dextral shear was applied in the *first phase* in all experiments by pulling the
 363 lower plastic sheet by 5 cm. In the *second phase* the left side of the experiment
 364 was extended by 3 cm orthogonally (BarMar6) or obliquely (315 degrees;
 365 BarMar 8 & 9) to the trend of the shear margin, whereas plate motion was
 366 reversed during the *third phase of deformation*, leading to inversion of earlier
 367 formed basins that had been



368 **Figure 3: A)** Schematic set-up of BarMar3-experiment as seen in map view. **B)**
 369 Section through same experiment before deformation, indicating stratification
 370 and thickness relations. **C)** Standard positions and orientation for sections cut in
 371 all experiments in the BarMar-series. Yellow numbers are section numbers.
 372 Black numbers indicate angle between the margins of the experiment (relative to
 373

374 N-S) for each profile. **D)** Outline of silicone putty layer as applied in all
 375 experiments. Inset shows original structural map of the Barents Margin used to
 376 define the width of the thinned crust. Red line (X-X') indicates the western limit
 377 of the thinned zone.
 378

379 developed in the strike-slip and extensional phases. Sedimentary basins that
 380 develop due to strike-slip (phase 1) or extension (phase 2) have been filled with
 381 layers of colored feldspar sand by sieving, so that a smooth surface was obtained.
 382 These layers are primarily important for discriminating among deformation
 383 phases and thus act as marker horizons. Phase 3 was initiated by inverting the
 384 orthogonal (BarMar6) or oblique (BarMar 8 & 9) extension of Phase 2 to
 385 contraction as a proxy for ridge-push that likely was initiated when the mid-



386
 387 **Figure 4:** Position of segments and major structural elements as referred to in
 388 the text and subsequent figures (see particularly **Figures 5 and 6**). This example
 389 is taken from the reference experiment BarMar6. All experiments BarMar6-9
 390 followed the same pattern, and the same nomenclature was used in the
 391 description of all experiments and provides the template for the definition of
 392 structural elements in **Figure 7**.
 393

394 oceanic ridge was established in Miocene time in the North Atlantic (Moser et al.,
 395 2002; Gaina et al., 2009). Contraction generated by ridge-push has been inferred
 396 from the mid Norwegian continental shelf (Våagnes et al., 1998; Pascal &
 397 Gabrielsen, 2001; Faleide et al., 2008; Gac et al., 2016) and seems still to prevail
 398 in the northern areas of Scandinavia (Pascal et al., 2005), although far-field

399 compression generated by other processes have been suggested (e.g. Doré &
400 Lundin, 1996).

401 Coloured layers of dry feldspar sand represent the brittle oceanic and
402 continental crust. This material has proven suitable for simulating brittle
403 deformation conditions (Willingshofer et al., 2005; Luth et al., 2010; Auzemery et
404 al., 2021). It is characterized by a grain size of 100-200 μm , a density of 1300
405 kgm^{-3} , a cohesion of $\sim 16\text{-}45$ Pa and a peak friction coefficient of 0.67
406 (Willingshofer et al., 2018). Additionally, a 8 mm thick and of variable width
407 corresponding to the transition zone (as mapped in reflection seismic data) of
408 'Rhodorsil Gomme GSIR' (Sokoutis, 1987) silicone putty mixed with fillers was
409 used as a proxy for the thinned and weakened continental crust at the ocean-
410 continent transition (**Figure 1B and 3A,B**). This Newtonian material ($n=1.09$)
411 has a density of 1330 kgm^{-3} and a viscosity of 1.42×10^4 Pa.s.

412 The experiments were scaled following standard scaling procedures as
413 described by Hubbert (1937), Ramberg (1967) or Weijermars and Schmelting
414 (1986), assuming that inertia forces are negligible when modelling tectonic
415 processes on geologic timescales (see Ramberg (1981) and Del Ventisette et al.
416 (2007) for a discussion on this topic). The models were scaled so that 10 mm in
417 the model approximates c. 10 km in nature yielding a length scale ratio of 1.00E-
418 6 . As such, the model oceanic and continental crusts scale to 18 and 26 km in
419 nature, respectively, which, although slightly overestimating the oceanic crustal
420 thickness (10-12 km) is in full agreement with the estimated thickness of the
421 thinned oceanward segment of the continental crust (30-20 km; Breivik et al.,
422 1998).

423 The brittle crust, dry feldspar sand, deforms according to the Mohr-
424 Coulomb fracture criterion (Horsfield, 1977; Mandl et al., 1977; McClay, 1990;
425 Richard et al., 1991; Klinkmüller et al., 2016), whereas silicone putty promotes
426 ductile deformation and folding. The configuration geometry applied in the
427 present experiments is accordingly well suited for the study of the COB in the
428 Barents Shear Margin (Breivik et al., 1998).

429 When complete, the experiments were covered with a thin layer of sand
430 further to stabilize the surface topography before the models were saturated
431 with water and cross-sections that were oriented transverse to the velocity

432 discontinuity were cut in a fan-shaped pattern (**Figure 3C**). All experiments have
433 been monitored with a digital camera providing top-view images at regular time
434 intervals of one minute.

435 All experiments performed were oriented in a N-S-coordinate framework
436 to facilitate comparison with the western Barents Sea area and had a three-stage
437 deformation sequence (dextral shear – extension – contraction). All descriptions
438 and figures relate to this orientation. It was noted that all experiments
439 reproduced comparable basic geometries and structural types, demonstrating
440 robustness against variations in contrasting strength of the “ocean-continent”-
441 transition zone, which included a zone of silicone putty with variable width
442 below an eastward thickening sand-wedge (**Figure 3B**). The experiments were
443 terminated before the full closure of the basin system, in accordance with the
444 extension vector > contraction vector as in the North Atlantic (see Vågnes et al.
445 1998; Pascal & Gabrielsen 2001; Gaina et al. 2009).

446

447 **Modelling Results**

448 A series of nine experiments (BarMar1-9) with the set-up described above was
449 performed. Experiments BarMar1-5 were used to calibrate and optimize
450 geometrical outline, deformation rate, and angles of relative plate movements
451 and are not shown here. The optimized geometries and experimental conditions
452 were utilized for experiments BarMar6-9, of which BarMar6 and 8 (and some
453 examples from BarMar9) are illustrated here. They yielded similar results in that
454 all crucial structural elements (faults and folds) were reproduced in all
455 experiments as described in the text (~~are shown in~~ **Figure 4**). It is emphasized
456 that the extensional basins affiliated with the extension phase (phase 2) were
457 wider for the orthogonal (BarMar6) as compared to the oblique extension
458 experiments (BarMar 8) (**Figures 5 and 6**). Furthermore, the fold systems
459 generated in the experiments that utilized oblique contraction of 315/135°
460 (BarMar8-9) produced more extensive systems of non-cylindrical folds. These
461 folds also had continuous, but more curved fold traces as compared to the
462 experiments with orthogonal extension/contraction (BarMar6). The fold axes
463 generally rotated to become parallel to the (extensional) master faults

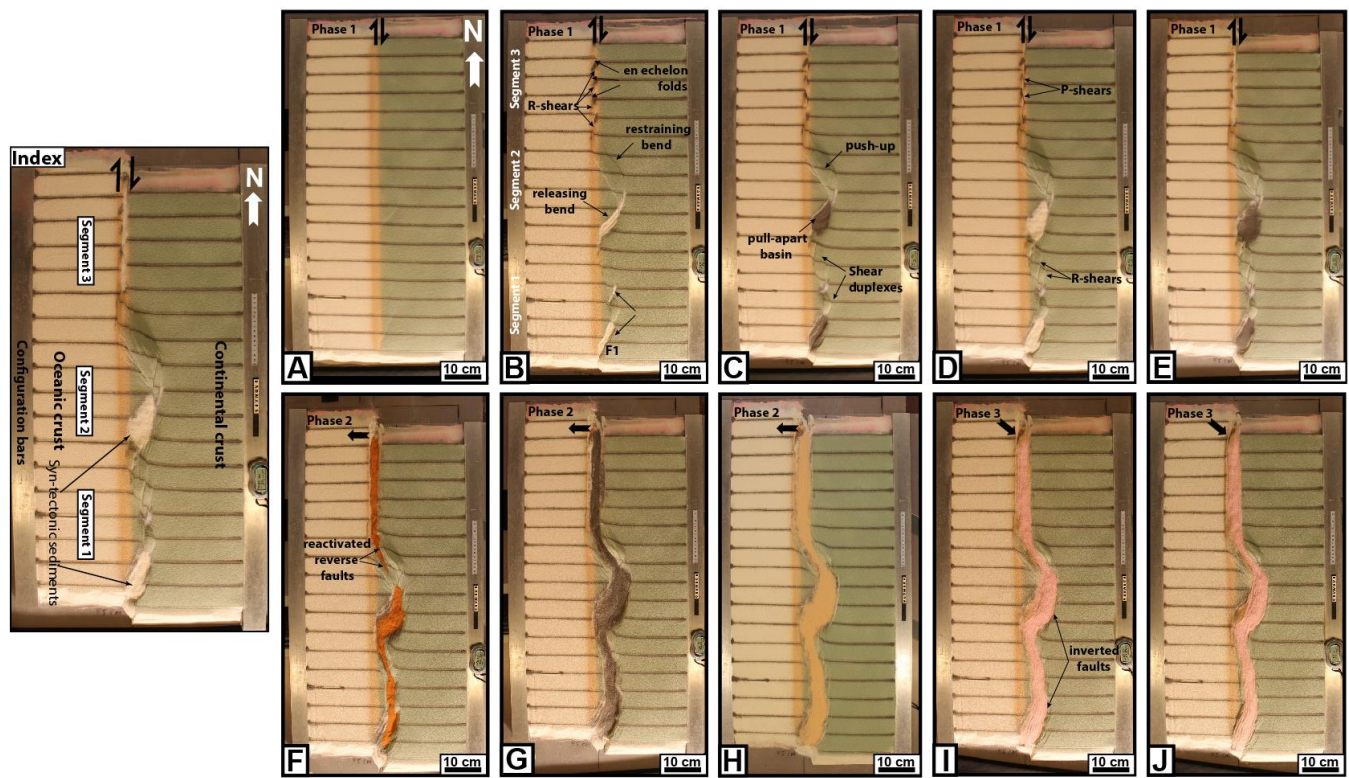
464 delineating the pull-apart basins generated in deformation stage 1 in
465 experiments with an oblique opening/closing angle.

466 Examples of the sequential development [are](#) displayed in **Figures 5 and**
467 **6**, and summarized in **Figure 7**. Elongated positive structural elements with
468 fold-like morphology as seen on the surface were detected during the various
469 stages of the present experiments. The true nature of those were not easily
470 determined until the experiments were terminated and transects could be
471 examined. Such structures included buried push-ups (*sensu* Dooley & Schreurs,
472 2012), antiformal stacks, back-thrusts, positive flower structures, fold trains, and
473 simple anticlines. For convenience, we use the non-genetic term “positive
474 structural elements” termed *PSEM-n* for such structure types as seen in the
475 experiments in the following description. In the following the deformation in
476 each segment is characterized for the three deformation phases (**Table 1**).

477 **Table 1**
 478 Characteristics of Positive Structural Element (PSE 1-6) as described in the text and shown in figures. Note that the PSE-1-structures
 479 that were developed in the earliest stages of the experiments became cannibalized during the continued deformation. No candidates of
 480 these structures were identified in the reflection seismic sections.
 481

Struct. type	Structural configuration	Orientation	Expr. stage	Segment	Recognized in seismic	Figure Expr	Figure Seism
PSE-1	Open syn-anticline system	135 deg	Stage 1	1,3	?	5,6	1A?
PSE-2	Incipient flower or half-flower	Parallel master fault	Stage 1	1,2,3	Yes	5,6,8	1B
PSE-3	Forced folds above rotated fault blocks	Parallel master fault in releasing bend	Stage 2	1,2	Yes	9B	
PSE-4	Push-up	Parallel master fault in restraining bend	Stage 1	2	Yes	9D	1C
PSE-5	Anticlines/snake-heads in hanging walls	Parallel master faults	Stage 3	1,2,3	Yes	9C,D	1D,E
PSE-6	Anticline-syncline trains	Parallel master faults	Stage 3	1,2,3	Yes	12	1F

482



483

484 **Figure 5:** Sequential development of experiment BarMar6 by 0.5, 2.4, 3.5, 4.0 and 5.0 cm of dextral shear (Steps A-E), orthogonal
 485 extension (steps F-H) and oblique contraction (steps I-J). The master fault strands are numbered in **Figure 4**, and the sequential
 486 development for each structural family is shown in **Figure 7**. The reference panel to the upper left shows the positions of the segments.

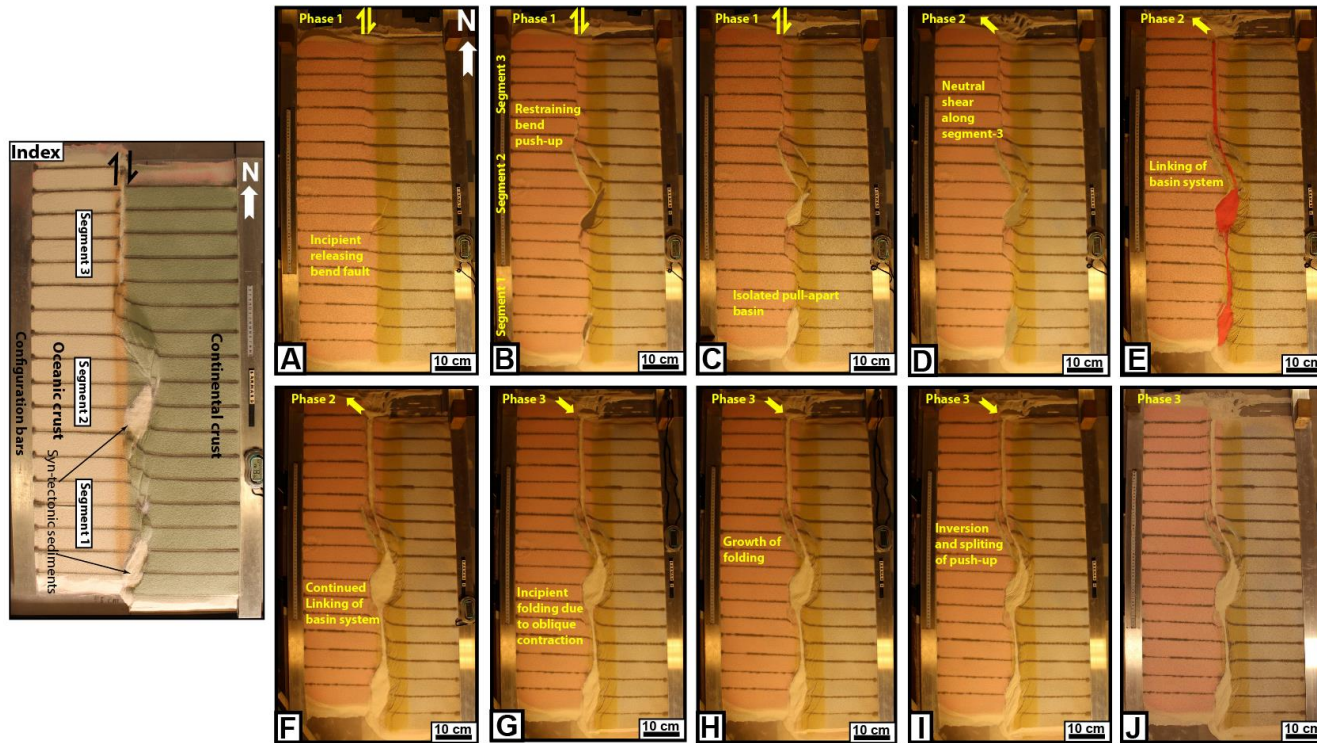
487 **Deformation phase 1: Dextral shear stage**

488 *Segment 1:* Differences in the geometry of the pre-cut fault trace between
489 segments 1, 2 and 3 became visible after the ~~first very initial~~ deformation stage.
490 ~~Particularly in~~ segments 1 and 3 in particular, an array of oblique *en échelon*
491 folds ~~in~~ between Riedel shear structures (*PSE-1-structures*) oriented c. 135°(NW-
492 SE) to the regional VD be came visible before rotating towards NNW-SSE by
493 continued shear (**Figure 8**; see also Wilcox et al., 1973; Ordonne & Vialon, 1983;
494 Richard et al., 1991; Dooley & Schreurs, 2012). These were simple, harmonic
495 folds with upright axial planes and fold axial traces extending a few cm beyond
496 the surface shear-zone described above. They had amplitudes on the scale of a
497 few millimeters and wavelengths on scale of 5 cm. The PSE-1-structures
498 interfered with or were dismembered by younger structures (Y-shears and PSE-
499 2-structures; see below) causing northerly rotation of individual intra-fault zone
500 lamellae (remnant PSE-1-structures; **Figure 8**). Structures similar to PSE-1-fold
501 arrays are known from almost all strike-slip experiments reported and described
502 in the literature (e.g. Cloos, 1928; Riedel, 1929; See Dooley & Schreurs, 2012 for
503 summary) and are therefore not given further attention here.

504 By 0.25 cm of horizontal displacement in segment 1, which included releasing
505 and restraining bends separated by a central strand of neutral shear, a slightly
506 curvilinear surface trace of a NE-SW-striking, top-NW normal fault in the
507 southernmost part of segment 1 developed. This co-existed with the PSE-1-
508 structures and became paralleled by a normal fault with opposite dip (fault 2,
509 **Figure 4**) so that the two faults constrained a crescent- or spindle-shaped
510 incipient extensional shear duplex (**Figures 5B and 6B**; see also Mann et al.,
511 1983).

512 A system of separate *en échelon* N-S to NNE-SSE-striking normal and
513 shear fault segments became visible in segment 1 after ca. 1 cm of shear (**Figure**
514 **5C,D**). These faults did not have the orientations as expected for R (Riedel) - and
515 R' (anti-Riedel)- shears (that would be oriented with angles of approximately 15
516 and 75° from the master fault trace) but became progressively linked with along
517 strike growth and the development of new faults and fault segments. They
518 thereby acquired the characteristics of Y-shears (oriented sub-parallel to the
519 master fault trace), dissecting the PSE-1-structures. By 2.4 cm of shear, segment

520 1 had become one unified fault array (**Figures 5D and 6D**), delineating a system
521 of incipient



522

523 **Figure 6:** Sequential development of experiment BarMar8 by 0.5, 2.4, 3.5, 4.0 and 5.0 cm of dextral shear (Steps A-E), oblique extension
 524 (steps F-H) and oblique contraction (steps I-J). The master fault strands are numbered in **Figure 3**, and the sequential development for
 525 each structural family is shown in **Figure 7**. Phases 2 and 3 involved oblique (315°) extension and contraction in this experiment. The
 526 reference panel to the upper left shows the positions of the segments.

527 push-ups or positive flower structures (*PSE-2-structures*; **Figures 8 and 10,**
528 **sections B1 and B3**).

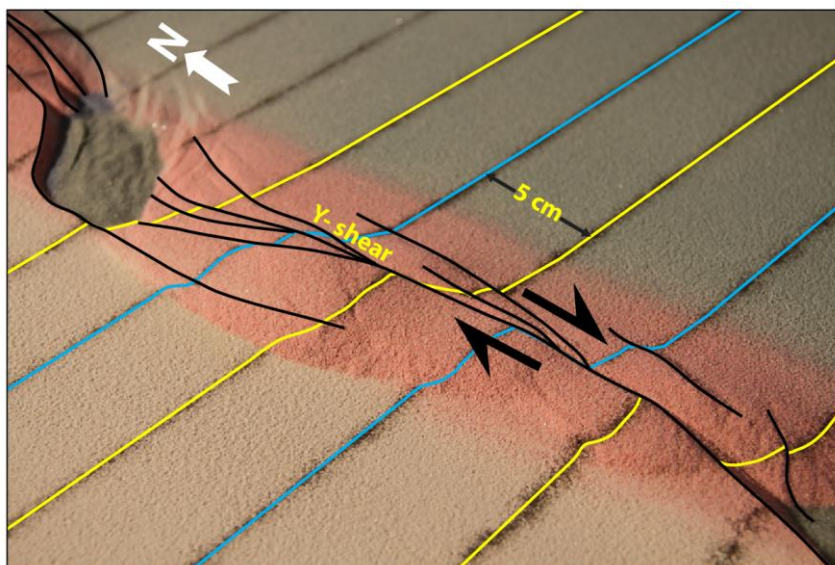
529 The PSE-2-structures had amplitudes of 1 - 2 cm and wavelengths of 3 - 5
530 cm as measured on the surface with fault surfaces that steepened down~~ward-~~
531 ~~section, with~~ the deepest parts of the structures having cores of sand-layers
532 deformed by open to tight folds. The folds had upright or slightly inclined axial
533 planes, dipping up to 55°, mainly to the east. The structures also affected the
534 shallowest layers down to 1-2 cm in the sequence, but the shallowest sequences
535 ~~were~~-developed at a later stage of deformation and were character~~ized~~ed by
536 simple gentle to open anticlines. These structures were constrained to a
537 deformation zone directly above the trace of the basement fault, similar to that
538 commonly seen along shear zones (e.g. Tchalenko, 1971; Crowell, 1974 a,b;
539 Dooley & Schreurs, 2012). This zone was 3-4 cm wide and remained stable
540 throughout deformation stage 1 and was restricted to the close vicinity of the
541 basement shear fault itself. A horse-~~tail~~-like fault array developed by ca. 3 cm of
542 shear at the transitions between segments 1 and 2 (**Figures 5B-D and 6B-D**).

543 The structuring in *Segment 2* was ~~determined~~ruled by the pre-cut
544 crescent-shaped basement fault (velocity discontinuity) ~~which~~that caused the
545 development of a releasing bend along its southern, and a restraining bend along
546 its northern border (**Figure 11**). The first fault of fault array 3a-e in the southern
547 part of Segment 2 (**Figure 4**) was activated after c. 0.15 cm of bulk horizontal
548 displacement (**Figure 7**). It was situated directly above the southernmost pre-cut
549 releasing bend, defining the margin of crescent-shaped incipient extensional
550 strike-slip duplexes (in the context of Woodcock & Fischer, 1986, Woodcock &
551 Schubert, 1994 and Twiss & Moores, 2007, p. 140-141). The developing basin got
552 a spindle-shaped structure and developed into a basin with a lazy-S-shape
553 (Cunningham & Mann, 2007; Mann, 2007). The basin widened towards the east
554 by stepwise footwall collapse, generating sequentially rotating crescent-shaped
555 extensional fault blocks that became trapped as extensional horses in the
556 footwall of the releasing bend (**Figure 11**). In the areas of the most pronounced
557 extension the crestal part of the rotational fault blocks became elevated above
558 the basin floor, generating ridges that influenced the basin floor topography and

559 hence, the sedimentation. By continued rotation of the fault blocks and
560 simultaneous sieving of sand the crests

566 of the blocks became sequentially uplifted, generating forced folds (Hamblin,
567 1965; Stearns, 1978; Groshong, 1989; Khalil & McClay, 2016) (**Figure 10A**). In
568 the analysis we used the term *PSE-3-structures* for these features.
569 Simultaneously, an expanding sand-sequence became trapped in the footwalls of
570 the master faults, defining typical growth-fault geometries.

571 By a shear displacement of 0.55 cm additional curved splay faults were
572 initiated from the northern tip of the master fault of fault 3f; **Figure 7**),
573 delineating the northern margin of a rhombohedral pull-apart-basin (Mann et al.,
574 1983; Mann, 2007; Christie-Blick & Biddle, 1985) and with a geometry that was
575 indistinguishable from pull-apart basins or rhomb grabens affiliated with
576 unbridged *en échelon* fault arrays (Crowell, 1974 a,b; Aydin & Nur, 1993).
577 Although sand was filled into the subsiding basins to minimize the graben relief



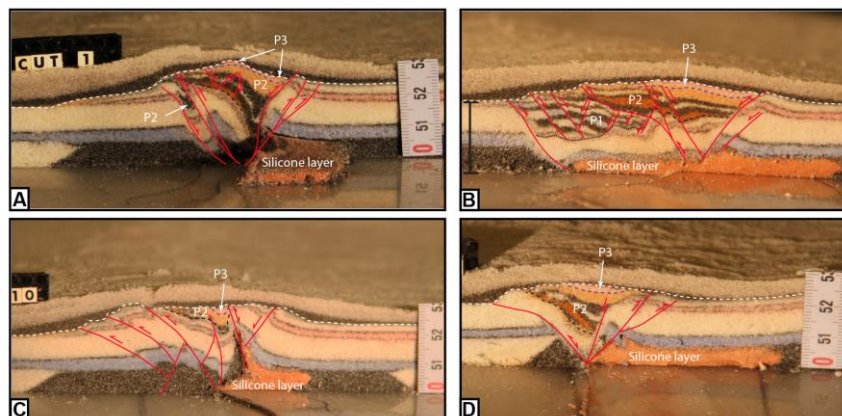
578
579 **Figure 8:** PSE-1 anticline-syncline pairs in segment 1 of experiment BarMar6 in
580 an oblique view (see **Figure 4** for position of Segment 1). PSE-1 folds (indicated
581 by relief defined by blue and yellow markers) were constrained to the central
582 fault zone (defined by Y-shear and its splay faults) and extended only 3-4 cm
583 beyond it. PSE-2 structures (incipient push-ups and positive flower structures)
584 were delineated by shear faults (black lines) and completely cannibalized PSE-1
585 structures by continued shear. Yellow and blue reference lines illustrate the
586 rotation of the fold axial trace caused by dextral shear. Already pre-shear
587 distance between the markers (blue and yellow lines) was 5cm. Black arrow
588 indicates shear direction.
589

590 and to prevent gravitational collapse, the sub-basins that were initiated in the
591 shear-stage were affected by internal cross-faults, and the initial basin units
592 remained the deepest so that the buried internal basin topography maintained a
593 high relief with several apparent depo-centers separated by intra-basinal
594 platforms. Systems of linked shear faults and PSE-structures became established
595 in the central part with neutral shear that separate the releasing and restraining
596 bends and development similarly to that seen for segment 3 (see below), ~~but~~ ~~the~~
597 ~~these~~ structures were, ~~however~~, soon destroyed by the interaction between the
598 northern and southern tips of the extensional and contractional shear duplexes
599 (**Figure 10**).

600 The first structure to develop in the regime of the restraining bend (segment 2;
601 was a top-to-the-southwest (antithetic) thrust fault at an angle of 145° with the
602 regional trend of the basement border as defined by segments 1 and 3 (Fault 6).
603 It became visible by 0.5 cm of displacement. ~~However~~, ~~The~~ northern part of
604 segment 2 became, ~~however~~, dominated by a synthetic contractional top-to-the-
605 northeast fault that was initiated by 0.85 cm of shear (Fault 7; **Figures 5 and 6**).
606 Thus, faults 6 and 7 delineated a growing half-crescent-shaped 5-7 -cm wide
607 push-up structure (Aydin & Nur, 1982; Mann et al., 1983) south of the
608 restraining bend (**Figure 9**; *PSE-4-structures*). ~~By~~ ~~continued~~ ~~shearing~~ ~~gave~~
609 these structures got the character of an antiformal stack.

610 *Segment 3* defined a straight strand of neutral shear. Its development in
611 the BarMar-experiments followed strictly that known from numerous published
612 experiments (e.g. Tchalenko, 1970; Wilcox et al., 1973; Harding, 1974; Harding &
613 Lowell, 1979; Naylor et al., 1986; Sylvester, 1988; Richard et al., 1991; Woodcock
614 & Schubert, 1994; Dauteuil & Mart, 1998; Mann, 2007; Casas et al., 2001; Dooley
615 & Schreurs, 2012). A train of Riedel-shears, occupying the full length of the
616 segment, appeared simultaneously on the surface after a shear displacement of
617 0.5 cm, occupying a restricted zone with a width of 2-3 cm. The Riedel-shears
618 dominated the continued structural development of Segment 3. Riedel'-shears
619 were absent throughout the experiments, as should be expected for a sand-
620 dominated sequence (Dooley & Schreurs, 2012). P-shears developed by
621 continued shear, creating linked rhombic structures delineated by the Riedel-
622 and P-shears generating positive structural elements with NW-SE- and NNE-SSE-

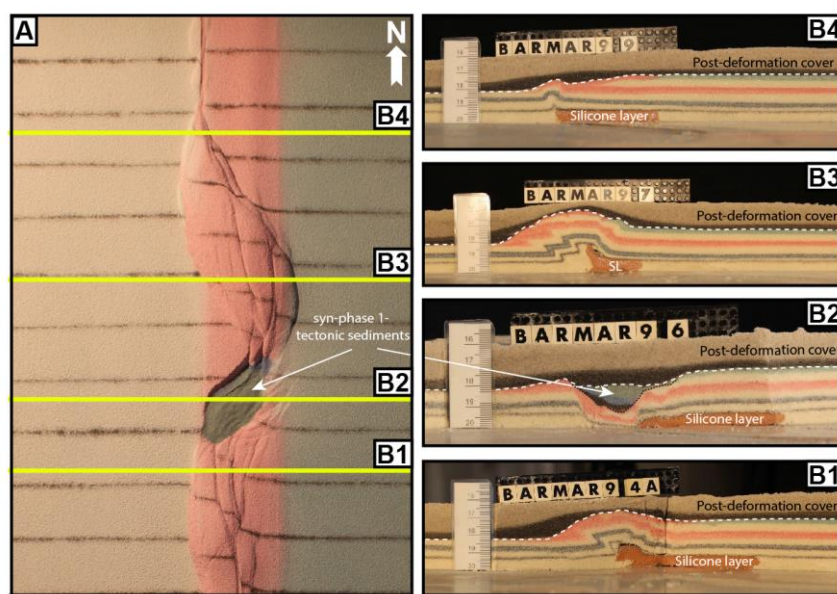
623 striking axes (see also Morgenstern & Tchalenko, 1967), soon coalescing to form
624 Y-shears.



625
626 **Figure 9:** Cross-sections through PSE-2-related structures. PSE-structures are
627 marked with P and PSE-number as described in text (see also Table 1). **A)**
628 Folded core of incipient push-up/positive flower structure in segment 1,
629 experiment BarMar6. The fold structure is completely enveloped of shear faults
630 that have a twisted along-strike geometry. Note that the eastern margin of the
631 structure developed into a negative structure at a late stage in the development
632 (filled by black-pink sand sequence) and that the silicone putty sequence (basal
633 pink sequence) was entirely isolated in the footwall. **B)** Similar structure type in
634 experiment BarMar8. However, the basal silicone putty layer here bridged the
635 basal high-strain zone so that folding occurred in the footwall as well as in the
636 hanging. Folds propagated up-section into the sand layers (blue). The folds in
637 upper (pink) layers are younger and were associated with the contractional stage
638 (PSE-6-structures). **C)** Contraction associated with “crocodile structure” in
639 the footwall of the main fault in segment 1, experiment BarMar8. Note
640 disharmonic folding with contrasting fold geometries in hanging wall and
641 footwall and at different stratigraphic levels in the footwall, indicating that
642 shifting stress situation in time and space occurred in the experiment. **D)**
643 Transitional fault strand between to more strongly sheared fault segments
644 (experiment BarMar9).
645

646 Transverse sections document that these structures were cored by push-up
647 anticlines, positive half-flower structures and full-fledged positive flower
648 structures in the advanced stages of shear (*PSE-4-structures*) (**Figures 5 and 6;**
649 **See also Figure 10**). These were accompanied by the development of *en échelon*
650 folds and flower structures as commonly reported from strike-slip faults in
651 nature and in experiments. The width of the zone above the basal fault remained
652 almost constant throughout the experiments, but was somewhat wider in

653 experiments with thicker basal silicone polymer layers, similar to that commonly
654 described from comparable experiments (e.g. Richard et al., 1991).
655



656
657 **Figure 10: A)** Contrasting structural styles along the master fault system in
658 segment 2 in map view and **(B)** cross sections of experiment BarMar9. SL
659 denotes silicone layer, the stippled line the boundary between pre- and syn-
660 deformation layers and the white dashed line the boundary with the post-
661 deformation layers.
662

663 **Deformation Phase 2: Extension**

664 The late Cretaceous-Palaeocene dextral shear was followed by pure extension
665 that accompanied the opening along the Barents Shear Margin in the Oligocene.
666 Our experiments focused on the effects of oblique extension, acknowledging that
667 plate tectonic reconstructions of the North Atlantic suggest an extension angle of
668 315° (Gaina et al., 2009).

669 All strike-slip basins widened in the extensional stage and as one would
670 expect, the basins generated in orthogonal extension became wider than those
671 generated in oblique extension. In both cases, however, extension promoted
672 enhanced relief that had been generated in the shear-stage. In the earliest
673 extensional stage, the strike-slip basin in segment 2 dominated the basin

674 configuration. By continued extension the linear segments and the minor pull-
675 apart basins in segments 1 and 2 started to open and became interlinked,
676 subsequently generating a linked basin system that runs parallel to the entire
677 shear margin (**Figures 5F-G, 6F-G**). The basins had become completely
678 interlinked by an extension of 1.25 cm (marked by the vertical dark blue line in
679 **Figure 7**). The orthogonal extension-phase also reactivated and linked several
680 master faults that were established in deformation phase 1 (**Figures 5A and**
681 **6A**). This became evident by an extension of 0.25 – 0.50 cm and included the
682 southern fault margin, the push-up and the splay faults defining the crestal
683 collapse graben (Faults 6, 11 and 12; **Figure 4**). Among the faults that remained
684 inactive throughout the extension phase were the antithetic contractional fault
685 delineating the push-ups in segment 2 (Fault 6; **Figure 4**). The Y-shear in
686 Segment 3 was reactivated as a straight, continuous extensional fault in phase 2.
687 Total extension in stage 2 was 5 cm.

688

689 **Deformation Phase 3: contraction**

690 In our experiments the extension stage was followed by oblique contraction (
691 parallel to the direction of extension as applied for each experiment). A part of
692 the early-stage contraction was accommodated along new faults. ~~It was more~~
693 ~~commonly,~~ however, ~~that~~ faults that had been generated in the strike-slip and
694 extensional stages became reactivated and rotated. ~~So was and~~ the development
695 of isolated folds, which were commonly associated with inverted fault traces,
696 generating snake-head or harpoon-structures structures (Cooper et al., 1989;
697 Coward, 1994; Allmendinger, 1998; Yameda & McClay, 2004; Pace & Calamitra,
698 2014; *PSE-5-structures*). The ~~predominant~~ structures affiliated with the
699 contractional stage ~~were~~ still new folds with traces oriented orthogonal to the
700 shortening direction and sub-parallel to the preexisting master fault systems
701 that defined the margin and basin margins (**Figure 12**). Also, some deep fold sets
702 that had been generated during the strike-slip phase and seen as domal surface
703 features became reactivated, causing renewed growth of surface structures (see
704 **Figure 10** and explanation in figure caption). These folds were generally up-
705 right cylindrical buckle folds in the initial contractional and with very large trace
706 ~~to length-~~ amplitude-ratio (*SPE-6-structures*). Some intra-basin folds, however,

707 defined fold arrays that crossed the basins in a diagonal fashion. Particularly the
708 folds situated along the basin margins developed into fault propagation-folds
709 above low-angle thrust planes. Such faults aligning the western basin margins
710 could have an antithetic attitude relative to the direction of contraction.

711 During the contractional phase the margin-parallel, linked basin system
712 started immediately to narrow and several fault strands became inverted. The
713 basin-closure was a continuous process until the end of the experiment by 3 cm
714 of contraction. The contraction was initiated as a proxy for an ESE-directed
715 ridge-push stage. The first effect of this deformation stage was heralded by uplift
716 of the margin of the established shear zone that had developed into a rift during
717 deformation stage 2. This was followed by the reactivation and inversion of
718 some master faults (e.g. fault a2; **Figure 4**) and thereafter by the development of
719 a new set of low-angle top-to-the-ESE contractional faults. These faults displayed
720 a sequential development (fault family 1; **Figure 7**) and were associated with
721 folding of the strata in the rift structure, probably reflecting foreland-directed in-
722 sequence thrusting (SPE-5 and PSE-6 fold populations).

723

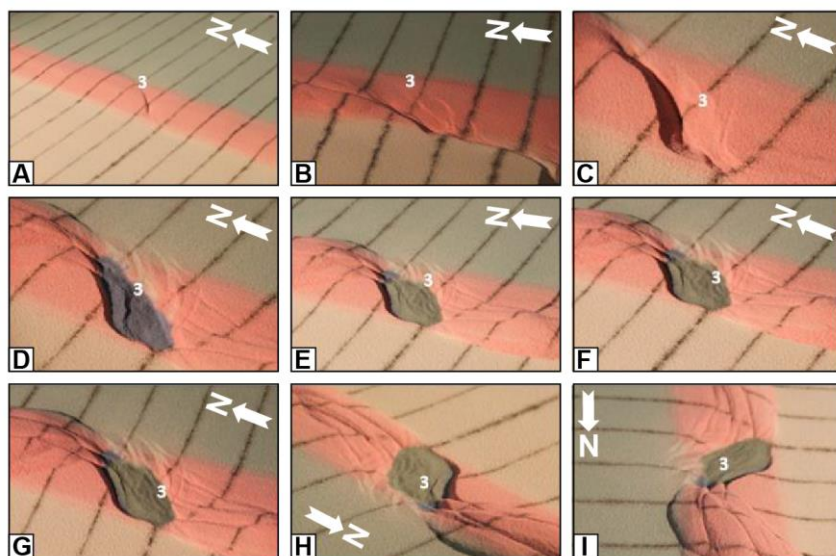
724 **Discussion**

725 The break-up and subsequent opening of the Norwegian-Greenland Sea was a
726 multi-stage event (**Figure 13**) that imposed shifting stress configurations
727 overprinting the already geometrically complex Barents Shear Margin.
728 Therefore, scaled experiments were designed to illuminate its structural
729 development. The experiments utilized three main segments that correspond to
730 the Senja Fracture Zone (segment 1), the Vestbakken Volcanic Province (segment
731 2) and the Hornsund Fault Zone (segment 3) respectively and three deformation
732 phases (dextral shear, oblique extension and contraction). Several structural
733 families (PSE 1-6) generated in the experiments correspond to structural
734 features observed in reflection seismic sections. In the following discussion we
735 utilize these two data sets in explaining the sequential development of each
736 segment of the shear margin.

737

738 **Structures of phase 1 (dextral shear)**

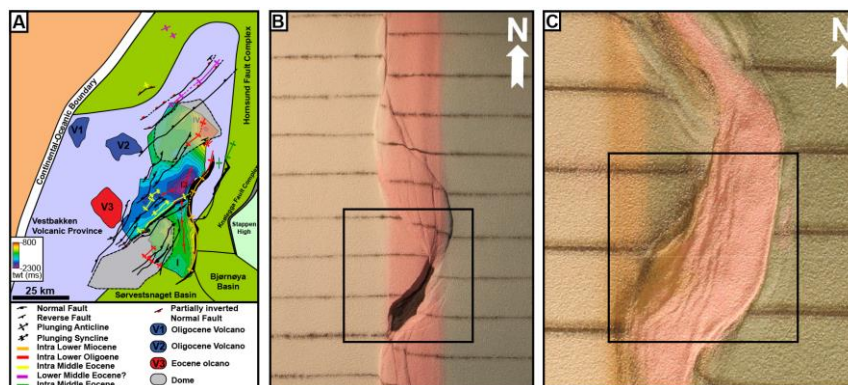
739 *Segment 1* (corresponding to the Senja Fracture Zone) was dominated by neutral
 740 dextral shear, although jogs in the (pre-cut) fault provided minor sub-segments
 741 with subordinate releasing and restraining bends.
 742 PSE-1-folds seen in the incipient shear phase were confined to the area just
 743 above the basal master fault (VD) and its immediate vicinity (see also
 744 experiments in



745
 746 **Figure 11:** Nine stages in the development of the extensional shear duplex
 747 system above the releasing bend in experiment BarMar9. The master faults that
 748 developed at an incipient stage (e.g. Fault 3 that constrained the eastern margin
 749 of the extensional shear duplex, marked with "3" in the figure; see also **Figure 7**)
 750 remained stable and continued to be active throughout the experiment, but
 751 became overstepped by new faults in its footwall. These were reactivated as
 752 contraction faults at the later stages (stages H and I in this figure). The
 753 developing basement was stabilized by infilling of gray sand during this part of
 754 the experiment. Fault 3 ~~continued to breach remained broke through~~ the basin
 755 infill also after the basin infill overstepped the original basin margin. The
 756 distance between the markers (dark lines) is 5cm. White arrow marks north-
 757 direction. Note that figures "H" and "I" (bottom right) is viewed from directions
 758 ~~than the other differs from the other figures figures.~~
 759

760 series "e" and "f" of Mitra & Paul, 2011). Counterparts to PSE-1 structural
 761 population were not identified in the seismic data, although some isolated, local
 762 anticlinal features could be dismembered remnants of such. Because of their
 763 constriction to the near vicinity of the master fault it is reasonable that

764 structures generated at an early stage of shear are vulnerable to cannibalization
 765 by younger structures with axes striking parallel to the main shear fault (Y-
 766 shears; SPE-2-structures). We therefore conclude that this structure population
 767 was destroyed during the later stages of shear and during the subsequent stages
 768 of extension and contraction.
 769



770
 771 **Figure 12:** PSE-5-folds generated during phase 3-inversion, experiment
 772 BarMar8. Note that fold axes are mainly parallel the basin rims, but that they
 773 deviate in some cases from that in the central parts of the basins, in some cases.
 774 The folds are best developed in segment 2, which accumulated extension in the
 775 combined shear and extension stages.
 776

777 PSE-1-folds that developed at an incipient stage were immediately pursued by
 778 the development of two sets of NNE-SSW-striking normal faults with opposite
 779 throws in the releasing bend areas (e.g. fault 2 **Figure 4**). The two faults defined
 780 crescent- or spindle-shaped incipient extensional shear duplexes. These
 781 structures were stable during the remainder of the experiments and their master
 782 faults became reactivated during the extensional and contractional phases (see
 783 below). The most prominent of these structures corresponds to the position of
 784 the Sørvestsnaget Basin (**Figure 1B**).

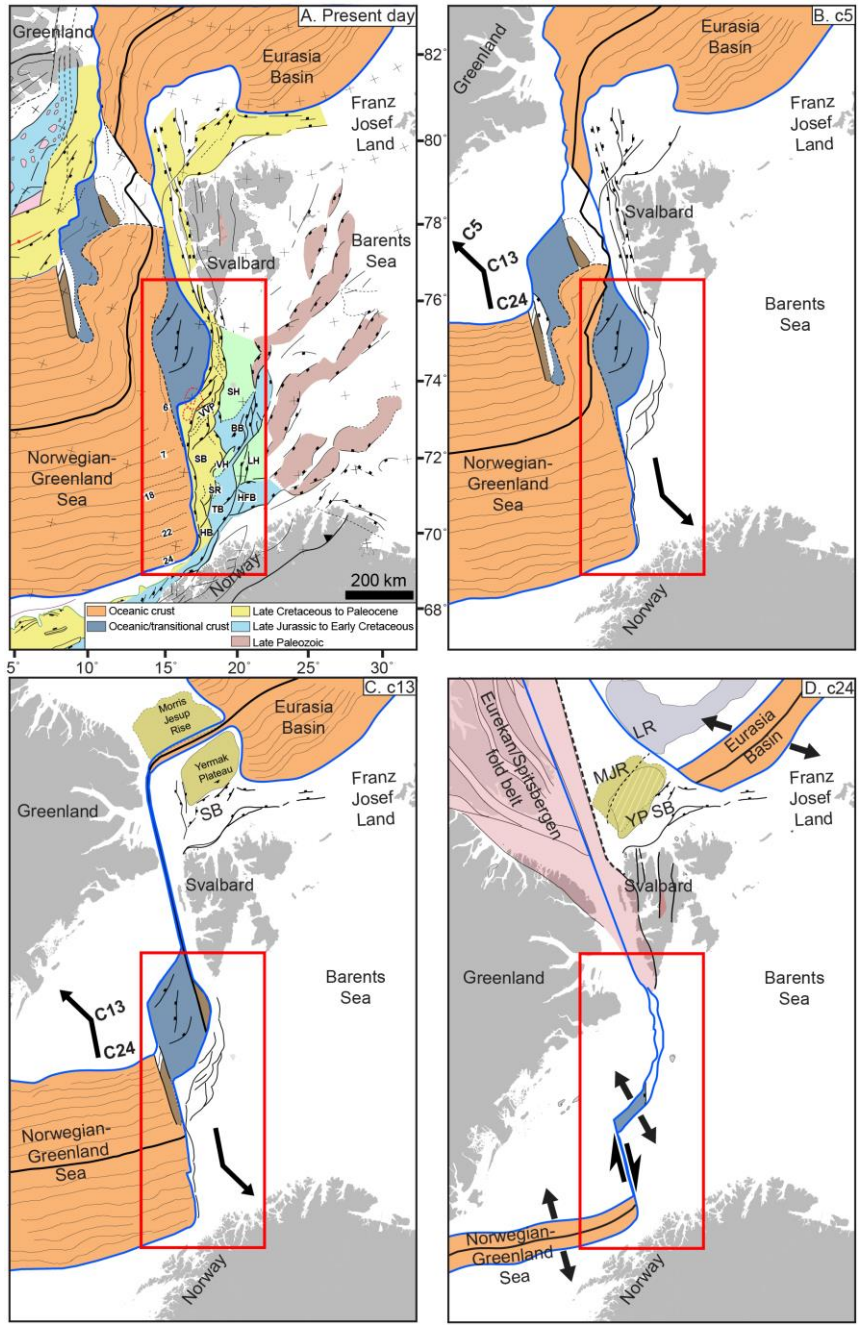
785 *Segment 2*, which was controlled by a pre-cut crescent-shaped
 786 discontinuity in the experiments corresponds to the Vestbakken Volcanic
 787 Province and the southern extension of the Knølegga Fault Complex of the
 788 Barents Shear Margin (**Figures 1B and 4**). The Vestbakken Volcanic Province is
 789 dominated by interfering NNW-SSE- and NE-SW striking fold- and fault systems
 790 in its central part, whereas N-S-structures are more common along its eastern

791 margin (**Figure 12A**) (Jebsen & Faleide, 1998; Giannenas, 2018). Intra-basinal
792 highs and other internal configurations seen in the BarMar-experiments mainly
793 reflect step-wise collapse of the intrinsic basin that generated rotational fault
794 blocks, the crests of which separated local sediment accumulations. Such
795 structures are common in strike-slip basins (e.g. Dooley & McClay, 1997; Dooley
796 & Schreurs, 2012) and are consistent with the intra-basin depo-centers seen
797 within the Vestbakken Volcanic province and in the Sørvestsnaget Basin as well
798 (Knutsen & Larsen, 1997; Jebsen & Faleide, 1998; **Figure 13**). The crests of the
799 rotating fault blocks are termed PSE-3-structures above, and such eroded fault
800 block crests are defining the footwalls of major faults in the Vestbakken Volcanic
801 Province, providing space for sediment accumulation in the footwalls. The area
802 that was affected by the basin formation in the extensional shear duplex stage
803 seems to have remained the deepest part of the Vestbakken Volcanic Province.
804 ~~Whereas the part formed by~~ basin widening ~~through~~ sequential footwall
805 collapse ~~formed~~ a shallower sub-platform (*sensu* Gabrielsen, 1986)
806 (**Figure 11**).

807 The Knølegga Fault Complex occupies a km-wide zone in segment 2. The
808 master fault strand is paralleled by faults with significant normal throws ~~in~~
809 hanging wall side and ~~is a part of this belongs to~~ the larger Knølegga Fault
810 Complex (EBF; Eastern Boundary Fault; Giannenas, 2018; **Figure 12A**). The EBF
811 zone is a top-west normal fault with maximum throw of nearly ~~2000 m~~ (3000
812 meters). It can be followed along its strike for more than 60 km and seems to die
813 out by horse-tailing at its tip-points. The vicinity of the master faults of the
814 Knølegga Fault Complex locally display isolated elongate positive structures
815 constrained by steeply dipping faults. These structures sometimes display
816 internal reflection patterns that seem exotic in comparison to the surrounding
817 sequences. Some of these structures resemble positive flower structures or
818 push-ups or define narrow anticlines. They are ~~located~~ found in both the footwall
819 and hanging wall of the ~~boundary~~ faults and strike parallel to ~~them~~
820 the axes of these structures ~~are~~ parallel the master faults. The traces of such
821 structures can be followed over shorter distances than the master faults, and do
822 not occur in the central parts of the Vestbakken Volcanic Province. We suggest
823 that the composite geometry of the Knølegga Fault Complex is due to the

824 development of PSE-2-structures within the realm of a pre-existing normal fault
825 zone.

826 Due to the right-stepping geometry during dextral shear in segment 2, the
827 southern and northern parts were in the releasing and restraining bend
828 positions, respectively (e.g. Christie-Blick & Biddle, 1985). Hence, the southern
829 part of segment 2 was subject to oblique extension, subsidence and basin
830 formation while the northern part was subject to oblique contraction, shortening
831 and uplift. The



832
 833 **Figure 13;** Main stages in opening of the North Atlantic. The figure builds on
 834 figure 5 in Faleide et al. (2008) and has been updated and redrawn.
 835

836 southern segment expanded to the east and northeast by footwall collapse and
837 activation of rotating fault blocks that contributed to a basin floor topography
838 that affected the pattern of sediment accumulation (**Figure 9A,B**).

839 The positive structural elements that prevail in *segment 3* belong to the
840 PSE-2-structure population. The structures affiliated with segment 3 in the
841 BarMar-experiments are similar to those seen in the reflection seismic sections
842 along parts of the Spitsbergen and the Senja shear margins (Myhre, et al. 1982)
843 and elsewhere (Cloos, 1928; Riedel, 1929; Tchalenko, 1970; Wilcox et al., 1973).
844 In the experiments *en echelon* folds (corresponding to PSE-1-structures) first
845 became visible, to be succeeded by the development of Riedel- and P-shears (R'-
846 shears were subdued as expected for sand-dominated sequences (Dooley &
847 Schreurs, 2012). Continued shear followed by collapse and interaction between
848 Riedel and P-shears and the subsequent development of Y-shears initiated push-
849 up- and flower-structure with N-S-axes (PSE-2) structures that were expressed
850 as non-cylindrical (double-plunging) anticlines on the surface (e.g. Tchalenko,
851 1970; Naylor et al., 1986). Structures similar to the PSE-2-structures that were
852 initiated in the present experiments are common in scaled experiments with
853 mechanically stratified sequences where viscous basal strata are covered by
854 sand (e.g. Richard et al., 1991; Dauteuil & Mart, 1998).

855

856 **Structures of phase 2 (extension)**

857 It is expected that (regional) basin and (local) fault block subsidence became
858 accelerated during phase 2 (extension), and more so in the orthogonal extension
859 experiments (BarMar 6) than in the experiments with oblique extension (BarMar
860 8). However, due to stabilization of basins by infilling of sand, this was not
861 documented in the final photographs. The widening occurred mainly by fault-
862 controlled collapse of the footwalls, and dominantly along the master faults that
863 correspond to the Knølegga Fault Complex. ~~However, new transverse fault~~
864 ~~within the basin that had developed during the, but also new intra-basin cross-~~
865 ~~faults that were initiated in the~~ shear stage (see above) ~~were also~~ became
866 reactivated ~~and,~~ contributing to the complexity of the basin topography. It is
867 ~~not~~ unlikely that a stage was reached where all (pull-apart) basin units along the

868 margin became fully linked, although sedimentary communication along the
869 margin may have ~~occurred~~become established.

870 During the oblique extension stage segment 1 of experiments BarMar7-9
871 the basin subsidence was focused in the minor pull-apart basins, which soon
872 became linked along the regional N-S-striking basin axis. Remains of several such
873 basin centers, of which the Sørvestsnaget Basin (Knutsen & Larsen, 1997;
874 Kristiansen et al., 2017) is the largest, are preserved and found in seismic data
875 (**Figure 1B**). During the experiments a continuous basin system was developed
876 in the hanging wall side of the master fault. It is, however, not likely that linking
877 of shear basins occurred prior to the opening stage along the Barents Shear
878 Margin.

879

880 **Structures of phase 3 (contraction)**

881 The contraction phase (phase 3) reactivated both normal and shear faults in the
882 master fault zone also causing folding in the hanging wall. Simultaneously
883 rotation of (intra-basinal) fault blocks and steepening of pre-existing faults
884 occurred. New fold populations (PSE-5-folds) with axial traces parallel to the
885 basin axis and the master faults characteri~~s~~ized the inversion stage. Remnants of
886 such folds are locally preserved in the thickest sedimentary sequences affiliated
887 with the Senja Shear Margin.

888 Fold systems with fold axes paralleling the basin margins as seen in the
889 experiments are also common in the Vestbakken Volcanic Province. Although
890 shortening occurred inside individual reactivated fault blocks by large
891 wavelength bulging of the entire sedimentary sequence also trains of folds with
892 larger amplitude and shorter wavelength were developed at this stage (**Figure**
893 **12B,C**). Thus, the tectonic inversion was focused along the N-S-striking basin
894 margins but also occurred along some pre-existing NE-SW-striking faults and in
895 the central parts of the basin.

896 During phase 3 the restraining bend configuration in the northern part of
897 segment 2 was characteri~~s~~zed by increasing contraction across strike-slip fault
898 strands that splayed out to the northwest from the central part of segment 2 in
899 an early stage of dextral shear. This deformation was terminated by the end of
900 phase 1 by stacking of oblique contraction faults (PSE-5 and PSE-6-structures),

901 defining an antiformal stack-like structure. This type of deformation falls outside
902 the mapped area, but to the north this type of oblique shortening during the
903 Eocene (phase 1) was accommodated by regional-scale strain partitioning
904 (Leever et al., 2011a,b).

905 Also, the Vestbakken Volcanic Province is characterized by extensive
906 regional shortening. Onset of this event of inversion/contraction is dated to early
907 Miocene (Jebsen & Faleide, 1998, Giannenas, 2018) and this deformation
908 included two main structural fold styles. The first includes upright to steeply inclined,
909 closed to open anticlines that are typically present in the hanging wall of master
910 faults. These folds typically have wavelengths in the order of 2.5 to 4.5 kilometers,
911 and amplitudes of several hundred meters. Most commonly they appear with head-on
912 snakehead-structures and are interpreted as buckle folds, albeit a component of shear
913 may occur in the areas of the most intense deformation. The second style includes
914 gentle to open anticline-syncline pairs with upright or steep to inclined axial planes
915 with wavelengths in the order of 5 to 7 kilometers and amplitudes of several tens of
916 meters to several hundred meters. We associate those with the PSE-4-type structures
917 as defined in the BarMar-experiments. These folds are situated in positions where
918 sedimentary sequences have been pushed against buttresses provided by master faults
919 along the basin margins. The PSE-6 folds developed as fold trains in the interior
920 basins, where buttressing against larger fault walls was uncommon. Also, this pattern
921 fits well with the development and geometry seen in the BarMar-experiments, where
922 folding started in the central parts of the closing basins before folding of the marginal
923 parts of the basin. In the closing stage the folding and inversion of master faults
924 remained focused along the basin margins.

925 The experiments clearly demonstrated that contraction by buckle folding
926 was the main shortening mechanism of the margin-parallel basin system
927 generated in phase 2 (orthogonal or oblique extension) in all segments. In the
928 Vestbakken Volcanic Province segments of the Knølegga Fault Complex, the EBF
929 and the major intra-basinal faults contain clear evidence for tectonic inversion,
930 whereas this is less pronounced in others. The hanging wall of the EBF is partly
931 affected by fish-hook-type inversion anticlines (Ramsey & Huber, 1987; Griera et
932 al., 2018) (**Figure 2D,E**), or isolated hanging wall anticlines or pairs or trains of
933 synclines and anticlines (e.g.; Roberts, 1989; Coward et al., 1991; Cartwright,

934 1989; Mitra, 1993; Uliana et al., 1995; Beauchamp et al. 1996; Gabrielsen et al.
935 1997; Henk & Nemcok 2008), the fold style and associated faults probably being
936 influenced by the orientation and steepness of the pre-inversion fault (Williams
937 et al., 1989; Cooper et al., 1989; Cooper & Warren, 2010). Some structures of this
938 type can still be followed for many kilometers having consistent geometry and
939 attitude. These structures ~~have are not been~~ much modified by reactivation and
940 are invariably found in the proximal parts footwalls of master faults, suggesting
941 that these are inversion structures. They correlate to PSE-type 5-structures in
942 the experiments that developed in areas of focused contraction along pre-
943 existing fault scarps during Oligocene inversion.

944 Trains of folds with smaller amplitudes and higher frequency are
945 sometimes found in fault blocks in the central part of the Vestbakken Volcanic
946 Province (**Figure 12A**). Although these structures ~~can are not be dated~~ by
947 seismic stratigraphical methods (on-lap configurations etc.) we assume
948 ~~that regard~~ these folds ~~can strains to~~ be correlated with the tight folds
949 generated in the inversion stage in the experiments (PSE-6-structures) and that
950 they are contemporaneous with the PSE-5-structures.

951 Segment 1 in the experiments, that corresponds to the Senja Shear Margin
952 , displays a structural pattern that is a hybrid between segments 1 and 2: It
953 contains incipient structural elements that were developed in full in segments 2
954 and 3, segment 2 being dominated by releasing and restraining bend
955 configurations and segment 3 dominated by neutral shear. ~~Because of~~Due to
956 internal configurations, the three segments were affected to secondary (oblique)
957 opening and contraction in various fashions. Understanding these differences
958 was much promoted by the comparison of seismic and model data.

959

960 **Some considerations about multiphase deformation in shear margins**

961 The Barents Shear Margin is a challenging target for structural analysis both
962 because it represents a geometrically complex structural system with a
963 multistage history, but also because high-quality (3D) reflection seismic data are
964 limited and many structures and sedimentary systems generated in the earlier
965 tectono-thermal stages have been overprinted and obliterated by younger
966 events. This makes analogue experiments very useful in the analysis, since they

967 offer a template for what kind of structural elements can be expected. By
968 constraining the experimental model according to the outline of the margin
969 geometry and ~~introducing~~~~imposing~~ a dynamic stress model ~~consistent with~~
970 ~~harmony~~ according to the ~~current understanding of the state-of-the-art~~
971 ~~knowledge about the regional~~ tectono-sedimentological ~~evolution~~~~development~~,
972 we were able to interpret the observations done ~~from the~~ reflection seismic
973 data in a new light.

974 Continental margins are commonly segmented containing primary or
975 secondary transform elements, and pure strike-slip transforms are relatively
976 rare (e.g. Nemcok et al. 2016). Such margins, however, invariably become
977 affected by extension following break-up and sometimes contraction due to
978 ridge-push or far-field stress perhaps related to plate reorganization. The
979 complexity of shear margins has ignited several conceptual discussions. One
980 such discussion concerns the presence of zones of weakness prior to break-up
981 (e.g. Sibuet & Mascle 1978; Taylor et al, 2009; Gibson et al. 2013; Basile 2015). In
982 the case of the Barents Shear Margin the de Geer zone provides such a pre-
983 existing zone of weakness, and this premise was acknowledged when the scaled
984 model was established. The relevance of our model is therefore constrained to
985 cases where a crustal-scale zone of weakness existed before break-up.
986 Furthermore, in cases with pre-existing zones of weakness, our model
987 ~~shows~~~~demonstrates~~ that the ~~initial~~~~ipient~~ architecture of the margin is ~~indeed~~
988 important indeed and the detailed geometry and width of the pre-existing weak
989 zone must be mapped and included in the model.

990

991 **Summary and conclusions**

992 Our observations confirmed that the main segments of the Barents Shear Margin,
993 albeit undergoing the same regional stress regime, display contrasting structural
994 configurations. The deformation in segment 2 in the BarMar-experiments, was
995 determined by releasing and restraining bends in the southern and northern
996 parts, respectively. Thus, the southern part, corresponding to the Vestbakken
997 Volcanic Province, was dominated by the development of a regional-scale
998 extensional shear duplex as defined by Woodcock & Fischer (1983) and Twiss &
999 Moores (2007). By continued shear the basin developed into a full-fledged pull-

1000 apart basin or rhomb graben (Crowell, 1974; Aydin & Nur, 1982) in which
1001 rotating fault blocks were trapped. The pull-apart-basin became the nucleus for
1002 greater basin systems to develop in the following phase of extension also
1003 providing the space for folds to develop in the contractional phase.

1004 We conclude that fault- and fold systems found in the realm of the
1005 Vestbakken Volcanic Province are in accordance with a three-stage development
1006 that includes dextral shear followed by oblique extension and contraction
1007 (315/135°) along a shear margin with composite geometry. Folds with NE-SW-
1008 trending fold axes are dominant in wider area of the Vestbakken Volcanic
1009 Province and are dominated by folds in the hanging walls of (older) normal
1010 faults, sometimes character~~ized~~ by narrow, snake-head- or harpoon-type
1011 structures that are typical for tectonic inversion (Cooper et al., 1989; Coward,
1012 1994; Allmendinger, 1998; Yameda & McClay, 2004; Pace & Calamitra, 2014).

1013 ~~Comparison of~~ seismic mapping and analogue experiments ~~shows it is~~
1014 ~~evident~~ that ~~one of the major~~ ~~main~~ challenges in analysing the structural
1015 pattern in shear margins of complex geometry and multiple reactivation is the
1016 low potential for preservation of structures ~~formed that were generated~~ in the
1017 earliest stages of ~~the~~ development.

1018
1019
1020
1021
1022
1023
1024
1025
1026
1027
1028
1029
1030
1031
1032

1033
1034
1035
1036
1037

1038 **Author contribution**

1039 R.H.Gabrielsen: Contributions to outline, design and performance of
1040 experiments. First writing and revisions of manuscript. First drafts of figures.

1041 P.A.Giannenas: Seismic interpretation in the Vestbakken Volcanic Province.
1042 Identification and description of fold families.

1043 Suggestion:

1044 D.Sokoutis: Main responsibility for set-up, performance and handling of
1045 experiments. Revisions of manuscript.

1046 E.Willigshofer: Performance and handling of experiments. Revisions of
1047 manuscript. Design and revisions of figure material.

1048 M. Hassaan: Background seismic interpretation. Discussions and revisions of
1049 manuscript. Design and revisions of figure material.

1050 J.I.Faleide: Regional interpretations and design of experiments. Participation in
1051 performance and interpretations of experiments. Revisions of manuscript,
1052 design and revisions of figure material.

1053

1054 **Acknowledgements**

1055 The work was supported by ARCEX (Research Centre for Arctic Petroleum
1056 Exploration), which was funded by the Research Council of Norway (grant
1057 number 228107) together with 10 academic and six industry (Equinor, Vår
1058 Energi, Aker BP, Lundin Energy Norway, OMV and Wintershall Dea) partners.
1059 Muhammad Hassaan was funded by the Suprabasins project (Research Council
1060 of Norway grant no. 295208). We thank to Schlumberger for providing us with
1061 academic licenses for Petrel software to do seismic interpretation. Two
1062 anonymous reviewers and the editors of this special volume provided comments,
1063 suggestions and advice that enhanced the clarity and scientific quality of the
1064 paper.

1065

1066
1067
1068
1069
1070
1071
1072
1073
1074
1075
1076
1077
1078
1079
1080
1081
1082
1083
1084
1085
1086
1087
1088
1089
1090
1091
1092
1093
1094
1095
1096
1097
1098
1099
1100
1101
1102
1103
1104
1105
1106
1107
1108
1109
1110
1111

References

- Allemand P. and Brun J.P.: Width of continental rifts and rheological layering of the lithosphere. *Tectonophysics*, 188, 63-69, 1991.
- Allmendinger, R.W.: : Inverse and forward numerical modeling of threeshear fault-propagation folds, *Tectonics*, 17(4), 640-656, 1998.
- Auzemery, A., E. Willingshofer, D. Sokoutis, J.P. Brun and Cloetingh S.A.P.L.: Passive margin inversion controlled by stability of the mantle lithosphere, *Tectonophysics*, 817, 229042, 1-17, <https://doi.org/10.1016/j.tecto.2021.229042>, 2021.
- Aydin, A. and Nur, A.: 1982: Evolution of pull-apart basins and their scale independence. *Tectonics*, 1, 91-105, 1982.
- Ballard J-F., Brun J-P and Van Ven Driessche J.: Propagation des chevauchements au-dessus des zones de décollement: modèles expérimentaux. *Comptes Rendus de l'Académie des Sciences, Paris*, 11, 305, 1249-1253, 1987.
- Basile, C.: Transform continental margins – Part 1: Concepts and models. *Tectonophysics*, 661, pp.1-10. doi: 10.1016/j.tecto.2015.08.034, 2015.
- Basile, C. and Brun, J.-P.: Transtensional faulting patterns ranging from pull-apart basins to transform continental margins: an experimental investigation, *Journal of Structural Geology*, 21, 23-37, 1997.
- Beauchamp, W., Barazangi, M., Demnati, A. and El Alji, M.: Intracontinental rifting and inversion: Missouri Basin and Atlas Mountains, Morocco. *American Association of Petroleum Geologists Bulletin*, 80(9), 1455-1482, 1996.
- Bergh, S.G., Braathen, A. and Andresen, A.: Interaction of basement-involved and thin-skinned tectonism in the Tertiary fold-and-thrust belt of Central Spitsbergen, Svalbard. *American Association of Petroleum Geologists Bulletin*, 81(4), 637-661, 1997.
- Bergh, S.G. and Grogan, P.: Tertiary structure of the Sørkapp-Hornsund Region, South Spitsbergen, and implications for the offshore southern extension of the fold-thrust belt. *Norwegian Journal of Geology*, 83, 43-60, 2003.

- 1112 Biddle, K.T. and Christie-Blick, N., (eds.): Strike-Slip Deformation, Basin
1113 Formation, and Sedimentation: Society of Economic Paleontologists and
1114 Mineralogists Special Publication, 37, 386pp, 1985a.
1115
1116 Biddle, K.T. and Christie-Blick, N.: Glossary — Strike-slip deformation, basin
1117 formation, and sedimentation, *in*: Biddle, K.T., and Christie-Blick, N. (eds.): Strike-
1118 Slip Deformation, Basin Formation, and Sedimentation: Society of Economic
1119 Paleontologists and Mineralogists Special Publication, 37, 375-386, 1985b
1120
1121 Blaich,O.A., Tsikalas,F. and Faleide,J.I.: New insights into the tectono-stratigraphic
1122 evolution of the southern Stappen High and the transition to Bjørnøya Basin, SW
1123 Barents Sea, Marine and Petroleum Geology, 85, 89-105, doi:
1124 10.1016/j.marpetgeo.2017.04.015, 2017.
1125
1126 Breivik,A.J., Faleide,J.I. and Gudlaugsson,S.T.: Southwestern Barents Sea margin:
1127 late Mesozoic sedimentary basins and crustal extension, Tectonophysics, 293, 21-44,
1128 1998.
1129
1130 Breivik,A.J., Mjelde,R., Grogan,P., Shinamura,H., Murai,Y. and Nishimura,Y.:
1131 Crustal structure and transform margin development south of Svalbard based on
1132 ocean bottom seismometer data. Tectonophysics, 369, 37-70 2003.
- 1133 Brekke, H.: The tectonic evolution of the Norwegian Sea continen- tal margin with
1134 emphasis on the Vøring and Møre basins: Geological Society, London, Special
1135 Publication, 136, 327–378, 2000.
- 1136 Brekke, H. and Riis, F.: Mesozoic tectonics and basin evolution of the Norwegian
1137 Shelf between 60°N and 72°N. Norsk Geologisk Tidsskrift, 67, 295-322, 1987.
1138
1139 Burchfiel, B.C. and Stewart,J.H.: "Pull-apart" origin of the central segment of Death
1140 Valley, California. Geological Society of America Bulletin, 77, 439-442, 1966.
1141
1142 Campbell,J.D.: *En échelon* folding, *Economical Geology*, 53(4), 448-472, 1958.
1143
1144 Cartwright,J.A.: The kinematics of inversion in the Danish Central Graben. *in*:
1145 M.A.Cooper & G.D.Williams (eds.): *Inversion Tectonics*. Geological Society of
1146 London Special Publication, 44, 153-175, 1989.
1147
1148 Casas, A.M., Gapals,D., Nalpas,T., Besnard,K. and Román-Berdiel,T.: Analogue
1149 models of transpressive systems, *Jornal of Structural Geology*, 23,733-743, 2001
1150
1151 Christie-Blick,N. and Biddle,K.T.: Deformation and basin formation along strike-slip
1152 faults. *in*: Biddle,K.T. & Christie-Blick,N. (eds.): *Strike-slip deformation, basin*
1153 *formation and sedimentation*. Society of Economic Mineralogists and
1154 *Palaeontologists (Tulsa Oklahoma)*, Special Publication, 37, 1-34, 1985.
1155
1156 Cloos,H.: Experimenten zur inneren Tectonick, *Zentralblatt für Mineralogie,*
1157 *Geologie und Palaentologie*, 1928B, 609-621, 1928.
1158
1159 Cloos,H.: Experimental analysis of fracture patterns, *Geological Society of America*

1160 Bulletin, 66(3), 241-256, 1955.
1161
1162 Cooper, M. and Warren, M.J.: The geometric characteristics, genesis and petroleum
1163 significance of inversion structures, in Law, R.D., Butler, R.W.H., Holdsworth, R.E.,
1164 Krabbendam, M. & Strachan, R.A. (eds.): Continental Tectonics and Mountain
1165 Building: The Legacy of Peache and Horne, Geological Society of London, Special
1166 Publication, 335, 827-846, 2010.
1167
1168 Cooper, M.A., Williams, G.D., de Graciansky, P.C., Murphy, R.W., Needham, T., de
1169 Paor, D., Stoneley, R., Todd, S.P., Turner, J.P. and Ziegler, P.A.: Inversion tectonics – a
1170 discussion. Geological Society, London, Special Publications, 44, 335-347, 1989.
1171
1172 Coward, M.: Inversion tectonics, in: Hancock, P.L. (ed.): Continental Deformation,
1173 Pergamon Press, 289-304, 1994.
1174
1175 Coward, M.P., Gillcrust, R. and Trudgill, B.: Extensional structures and their tectonic
1176 inversion in the Western Alps, *in*: A.M. Roberts, G. Yielding & B. Freeman (eds.): The
1177 Geometry of Normal Faults. Geological Society of London Special Publication, 56,
1178 93-112 1991.
1179
1180 Crowell, J.C.: Displacement along the San Andreas Fault, California, Geological
1181 Society of America Special Papers, 71, 59pp, 1962.
1182
1183 Crowell, J.C.: Origin of late Cenozoic basins in southern California. in Dorr, R.H. and
1184 Shaver, R.H. (eds.): Modern and ancient geosynclinal sedimentation. SEPM Special
1185 Publication, 19, 292-303, 1974a
1186
1187 Crowell, J.C., 1974b: Implications of crustal stretching and shortening of coastal
1188 Ventura Basin, *in*: Howell, D.G. (ed.): Aspects of the geological history of the
1189 California continental Borderland, American Association of Petroleum Geologists,
1190 Pacific Section, Publication, 24, 365-382, 1974b
1191
1192 Cunningham, W.D. and Mann, P. (eds.): : Tectonics of Strike-Slip Restraining and
1193 Releasing Bends, Geological Society London Special Publication, 290, 482pp, 2007a.
1194
1195 Cunningham, W.D. and Mann, P.: Tectonics of Strike-Slip Restraining and Releasing
1196 Bends, *in*: Cunningham, W.D. & Mann, P. (eds.), 2007: Tectonics of Strike-Slip
1197 Restraining and Releasing Bends, Geological Society London Special Publication,
1198 290, 1-12, 2007b.
1199
1200 Dauteuil, O. and Mart, Y.: Analogue modeling of faulting pattern, ductile
1201 deformation, and vertical motion in strike-slip fault zones, Tectonics, 17(2), 303-310,
1202 1998.
1203
1204 Del Ventisette, C., Montanari, D., Sani, F., Bonini, M. and Corti, G.: Reply to
1205 comment by J. Wickham on ‘‘Basin inversion and fault reactivation in laboratory
1206 experiments’’. Journal of Structural Geology 29, 1417–1418, 2007.
1207
1208 Dooley, T. and McClay, K.: Analog modeling of pull-apart basins, American
1209 Association of Petroleum Geologists Bulletin, 81(11), 1804-1826, 1997.

1210
1211 Dooley, T.P. and Schreurs, G.: Analogue modelling of intraplate strike-slip tectonics:
1212 A review and new experimental results, *Tectonophysics*, 574-575, 1-71, 2012
1213
1214 Doré, A.G. and Lundin, E.R.: Cenozoic compressional structures on the NE Atlantic
1215 margin: nature, origin and potential significance for hydrocarbon exploration.
1216 *Petroleum Geosciences*, 2, 299-311, 1996
1217
1218 Doré, A.G., Lundin, E.R., Gibbons, A., Sømme, T.O. and Tørudbakken, B.O.:
1219 Transform margins of the Arctic: a synthesis and re-evaluation *in*: Nemcok, M.,
1220 Rybár, S., Sinha, S.T., Hermeston, S.A. & Ledvényiová, L. (eds.): *Transform Margins*:
1221 Development, Control and Petroleum Systems, Geological Society London, Special
1222 Publication, 431, 63-94, 2016.
1223
1224 Doré, A.G., Lundin, E.R., Jensen, L.N., Birkeland, Ø., Eliassen, P.E. and Fichler, C.:
1225 Principal tectonic events in the evolution of the northwest European Atlantic margin.
1226 In: A.J. Fleet & S.A.R. Boldy (eds.): *Petroleum Geology of Northwest Europe*:
1227 Proceedings of the Fifth Conference (Geological Society of London), 41-61, 1999.
1228
1229 Eidvin, T., Goll, R.M., Grogan, P., Smelror, M. and Ulleberg, K.: The Pleistocene to
1230 Middle Eocene stratigraphy and geological evolution of the western Barents Sea
1231 continental margin at well site 731675-1 (Bjørnøya West area). *Norsk Geologisk*
1232 *Tidsskrift*, 78, 99-123 1988.
1233
1234 Eidvin, T., Jansen, E. and Riis, F.: Chronology of Tertiary fan deposits off the western
1235 Barents Sea: Implications for the uplift and erosion history of the Barents Shelf.
1236 *Marine Geology*, 112, 109-131, 1993.
1237
1238 Eldholm, O., Faleide, J.I. and Myhre, A.M.: Continent-ocean transition at the western
1239 Barents Sea/Svalbard continental margin. *Geology*, 15, 1118-1122, 1987.
1240
1241 Eldholm, O., Thiede, J., and Taylor, E.: Evolution of the Vøring volcanic margin, *in*:
1242 Eldholm, O., Thiede, J., and Taylor, E., (eds.): *Proceedings of the Ocean Drilling*
1243 *Program, Scientific Results*, 104: College Station (Ocean Drilling Program), TX,
1244 1033-1065, 1989.
1245
1246 Eldholm, O., Tsikalas, F. and Faleide, J.I.: Continental margin off Norway 62-
1247 75°N: Paleogene tectono-magmatic segmentation and sedimentation. *Geological*
1248 *Society of London Special Publication*, 197, 39-68, 2002
1249
1250 Emmons, R.C.: Strike-slip rupture patterns in sand models, *Tectonophysics*, 7, 71-87,
1251 1969.
1252
1253 Faugère, E., Brun, J.-P. and Van Den Driessche, J.: Bassins asymétriques en
1254 extension pure et en détachements: Modèles expérimentaux, *Bulletin Centre*
1255 *Recherche Exploration et Production Elf Aquitaine*, 10(2), 13-21, 1986.
1256
1257 Faleide, J.I., Bjørlykke, K. and Gabrielsen, R.H.: Geology of the Norwegian Shelf. *in*:
1258 Bjørlykke, K.: *Petroleum Geoscience: From Sedimentary Environments to Rock*
1259 *Physics 2nd Edition*, Springer-Verlag, Berlin Heidelberg, Chapter 25, 603 -637, 2015.

- 1260
1261 Faleide, J.I., Myhre, A.M. and Eldholm, O.: Early Tertiary volcanism at the western
1262 Barents Sea margin. in: A.C.Morton & L.M.Parsons (eds.): Early Tertiary volcanism
1263 and the opening of the NE Atlantic.Geological Society of London Special Publication,
1264 39,135-146, 1988.
1265
1266 Faleide, J.I., Tsikalas, F., Breivik, A.J, Mjelde, R., Ritzmann, O., Engen, Ø., Wilson,
1267 J. and Eldholm, O.: Structure and evolution of the continental margin off Norway and
1268 the Barents Sea. Episodes, 31(1), 82-91, 2008.
1269
1270 Faleide, J.I., Vågnes, E. and Gudlaugsson, S.T.: Late Mesozoic - Cenozoic evolution
1271 of the south-western Barents Sea in a regional rift-shear tectonic setting. Marine and
1272 Petroleum Geology, 10, 186-214, 1993
1273
1274 Fichler, C. and Pastore, Z.: Petrology and crystalline crust in the southwestern Barents
1275 Sea inferred from geophysical data. Norwegian Journal of Geology, 102, 41pp,
1276 <https://dx.doi.org/10.17850/njg102-2-2>, 2022.
1277
1278 Freund, R.: The Hope Fault, a strike-slip fault in New Zealand, New Zealand
1279 Geological Survey Bulletin, 86, 1-49, 1971.
1280
1281 Gabrielsen, R.H.: Structural elements in graben systems and their influence on
1282 hydrocarbon trap types. in: A.M. Spencer (ed.): Habitat of Hydrocarbons on the
1283 Norwegian Continental Shelf. Norw. Petrol. Soc. (Graham & Trotman), 55 – 60,
1284 1986.
1285
1286 Gabrielsen, R.H., Færseth, R.B., Jensen, L.N., Kalheim, J.E. and Riis, F.: Structural
1287 elements of the Norwegian Continental Shelf. Part I: The Barents Sea Region.
1288 Norwegian Petroleum Directorate, Bulletin, 6, 33pp, 1990.
1289
1290 Gabrielsen, R.H., Grunnaleite, I. and Rasmussen, E.: Cretaceous and Tertiary
1291 inversion in the Bjørnøyrenna Fault Complex, south-western Barents Sea. Marine and
1292 Petroleum Geology, 142, 165-178, 1997.
1293
1294 Gac, S., Klitzke, P., Minakov, A., Faleide, J.I. and Scheck-Wenderoth, M.,:
1295 Lithospheric strength and elastic thickness of the Barents Sea and Kara Sea region,
1296 Tectonophysics, 691, 120-132, doi: 10.106/j.tecto.2016.04.028, 2016.
1297
1298 Gaina, C., Gernigon, L. and Ball.P.: Palaeocene – Recent plate boundaries in the NE
1299 Atlantic and the formation of the Jan Mayen microcontinent. Journal of the
1300 Geological Society, London, 166(4), 601-616, 2009.
- 1301 Ganerød, M., Smethurst, M.A., Torsvik, T.H., Prestvik, T., Rouse, S., McKenna, C.,
1302 van Hinsbergen, D.J.J. and Hendriks, W.W.H.: The North Atlantic Igneous Province
1303 reconstructed and its relation to the Plume Generation Zone: the Antrim Lava Group
1304 revisited. Geophysical Journal International, 182, 183-202, doi: 10.1111/j.1365-
1305 246X.2010.04620.x, 2010.
- 1306 Giannenas, P.A.: The Structural Development of the Vestbakken Volcanic Province,
1307 Western Barents Sea. Relation between Faults and Folds, Unpublished Ms.Sci.thesis,

1308 University of Oslo, 89 pp., 2018
1309
1310 Gibson, G.M., Totterdell, J.M., White, N. Mitchell, C.H., Stacey, A.R., M. P. Morse,
1311 M.P. and A. Whitaker: Preexisting basement structures and its influence on
1312 continental rifting and fracture development along Australia's southern rifted margin,
1313 *Journal of the Geological Society of London*, 170, 365-377, 2013.
1314 .
1315
1316 Graymer, R.W., Langenheim, V.E., Simpson, R.W., Jachens, R.C. and Ponce, D.A.:
1317 Relative simple through-going fault planes at large-earthquake depth may be
1318 concealed by surface complexity of strike-slip faults, *in*: Cunningham, W.D. &
1319 Mann, P. (eds.): *Tectonics of Strike-Slip Restraining and Releasing Bends*, Geological
1320 Society London Special Publication, 290, 189-201, 2007.
1321
1322 Griera, A., Gomez Rivas, E. and Llorens, M.-G.: The influence of layer-interface
1323 geometry of single-layer folding. *Geological Society of London Special Publication*
1324 487, SP487:4, 2018.
1325
1326 Grogan, P., Østvedt-Ghazi, A.-M., Larssen, G.B., Fotland, B., Nyberg, K., Dahlgren,
1327 S. and Eidvin, T.: Structural elements and petroleum geology of the Norwegian sector
1328 of the northern Barents sea. *in*: Fleet, A.J. & Boldry, S.A.R. (eds.): *Petroleum Geology*
1329 *of Northwest Europe: Proceedings of the 5th Conference*, Geological Society of
1330 London, 247-259, 1999.
1331
1332 Groshong, R.H.: Half-graben structures: balanced models of extensional fault
1333 bend folds, *Geological Society of America Bulletin*, 101, 96-195, 1989
1334
1335 Gudlaugsson, S.T. and Faleide, J.I.: The continental margin between Spitsbergen &
1336 Bjørnøya, *in*: O.Eiken (ed.): *Seismic Atlas of Western Svalbard*, Norsk Polarinstitutt
1337 Meddelelser, 130, 11-13, 1994.
1338
1339 Gudlaugsson, S.T., Faleide, J.I., Johansen, S.E. and Breivik, A.J.: Late Palaeozoic
1340 structural development of the south-western Barents Sea. *Marine and Petroleum*
1341 *Geology*, 15, 73-102, 1998.
1342
1343 Hamblin, W.K.: Origin of "reverse drag" on the down-thrown side of normal
1344 faults, *Geological Society of America Bulletin*, 76, 1145-1164, 1965.
1345
1346 Hanisch, J.: The Cretaceous opening of the Northeast Atlantic. *Tectonophysics*, 101,
1347 1-23, 1984.
1348
1349 Harding, T.P.: Petroleum traps associated with wrench faults. *American Association*
1350 *of Petroleum Geologists Bulletin*, 58, 1290-1304, 1974.
1351
1352 Harding, T.P. and Lowell, J.D.: Structural styles, their plate tectonic habitats, and
1353 hydrocarbon traps in petroleum provinces, *American Association of Petroleum*
1354 *Geologists Bulletin*, 63, 1016-1058, 1979.
1355
1356 Harland, W.B.: The tectonic evolution of the Arctic-North Atlantic Region, *in*:
1357 Taylor, J.H., Rutten, M.G., Hales, A.L., Shackleton, R.M., Nairn, A.E. & Harland, W.B.:

- 1358 Discussion, A Symposium on Continental Drift, Philosophical Transactions of the
 1359 Royal Society of London,, Series A, 258, 1088, 59-75, 1965.
 1360
- 1361 Harland, W.B.: Contributions of Spitsbergen to understanding of tectonic evolution of
 1362 North Atlantic Region, American Association of Petroleum Geologists, Memoir 12,
 1363 817-851, 1969.
 1364
- 1365 Harland, W.B.: Tectonic transpression in Caledonian Spitsbergen, Geological
 1366 Magazine, 108, 27-42, 1971
 1367
- 1368 Henk, A. and Nemcok, M.: Stress and fracture prediction in inverted half-graben
 1369 structures. Journal of Structural Geology, 30(1), 81-97, 2008.
- 1370 Horni, J.Á., Hopper, J.R., Blischke, A., Geisler, W.H., Stewart, M., Mcdermott, K.,
 1371 Judge, M., Erlendsson, Ö. and Ártíng, U.E.: Regional Distribution of Volcanism
 1372 within the North Atlantic Igneous Province. The NE Atlantic Region: A Reappraisal
 1373 of Crustal Structure, Tectonostratigraphy and Magmatic Evolution. Geological
 1374 Society, London, Special Publications, 447, 105-125,
 1375 <https://doi.org/10.1144/SP447.18>, 2017.
- 1376 Horsfield, W.T., 1977: An experimental approach to basement-controlled
 1377 faulting. Geologie en Mijnbouw, 56(4), 3634-370 1977.
 1378
- 1379 Hubbert, M.K.: Theory of scale models as applied to the study of geologic
 1380 structures, Bulletin Geological Society of America, 48, 1459-1520, 1937.
- 1381 Jepsen, C. and Faleide, J.I.: Tertiary rifting and magmatism at the western Barents
 1382 Sea margin (Vestbakken volcanic province). III international conference on Arctic
 1383 margins, ICAM III; abstracts; plenary lectures, talks and posters, 92, 1998.
- 1384 Khalil,S.M. and McClay,K.R.: 3D geometry and kinematic evolution of extensional
 1385 fault-related folds, NW Red Sea, Egypt. in: Childs,C., Holdswort,R.E.,
 1386 Jackson,C.A.L., Manzocchi,T., Walsh,J.J & Yielding,G. (eds.): The Geometry and
 1387 Growth of Normal Faults, Geological Society, London, Special Publication 439,
 1388 doi.org/10.1144/SP439.11, 2016.
 1389
- 1390 Klinkmüller, M., Schreurs, G., Rosenau, M. and Kemnitz, H.: Properties of
 1391 granular analogue model materials: a community wide survey. Tectonophysics
 1392 684, 23-38. <http://dx.doi.org/10.1016/j.tecto.2016.01.017.feb>, 2016.
 1393
- 1394 Knutsen, S.-M. and Larsen,K.I.: The late Mesozoic and Cenozoic evolution of the
 1395 Sørvestsnaget Basin: A tectonostratigraphic mirror for regional events along the
 1396 Southwestern Barents Sea Margin? Marine and Petroleum Geology, 14(1), 27-54,
 1397 1997.
 1398
- 1399 Kristensen, T.B., Rotevatn, A., Marvik, M., Henstra, G.A., Gawthorpe, R.L. and
 1400 Ravnås, R.: Structural evolution of sheared basin margins: the role of strain
 1401 partitioning. Sørvestsnaget Basin, Norwegian Barents Sea, Basin Research, (2017), 1-
 1402 23, doi:10.1111/bre.12235, 2017.
 1403

- 1404 Le Calvez, J-H. and Vendeville, : Experimental designs to mode along strike-slip fault
 1405 interaction. *in*: Scellart, W.P. & Passcheir, C. (eds.). Analogue Modeling of large-
 1406 scale Tectonic Processes, Journal of Virtual Explorer, 7, 7-23, 2002.
 1407
- 1408 Leever, K.A., Gabrielsen, R.H., Sokoutis, D. and Willingshofer, E.: The effect of
 1409 convergence angle on the kinematic evolution of strain partitioning in transpressional
 1410 brittle wedges: insight from analog modeling and high resolution digital image
 1411 analysis. *Tectonics*, 30, TC2013, 1-25, doi: 10.1029/2009TC002649, 2011a.
 1412
- 1413 Leever, K.A., Gabrielsen, R.H., Faleide, J.I. and Braathen, A.: A transpressional
 1414 origin for the West Spitsbergen Fold and Thrust Belt - insight from analog modeling.
 1415 *Tectonics*, 30, TC2014, 1- 24, doi: 10.1029/2010TC002753, 2011b.
 1416
- 1417 Libak, A., Mjelde, R., Keers, H., Faleide, J.I. and Murai,Y.: An intergrated
 1418 geophysical study of Vestbakken Volcanic Province, western Barents Sea continental
 1419 margin, and adjacent oceanic crust, *Marine Geophysical Research*, 33(2), 187-207,
 1420 2012.
 1421
- 1422 Lorenzo, J.M.: Sheared continental margins: an overview, *Geo-Marine Letters*, 17(1),
 1423 1-3, 1997
- 1424 Lowell, J.D., 1972: Spitsbergen Tertiary orogenic belt and the Spitsbergen fracture
 1425 zone, *Geol. Soc. Am. Bull.*, 83, 3091–3102, doi:10.1130/0016-
 1426 7606(1972)83[3091:STOBAT]2.0.CO;2, 1972.
- 1427 Lundin, E.R. and Doré, A.G.: A tectonic model for the Norwegian passive margin
 1428 with implications for the NE Atlantic.: Early Cretaceous to break-up. *Journal of the*
 1429 *Geological Society London*, 154, 545-550, 1997.
 1430
- 1431 Lundin, E.R., Doré, A.G., Rønning, K. and Kyrkjebø, R.: Repeated inversion in the
 1432 Late Cretaceous-Cenozoic northern Vøring Basin, offshore Norway, *Petroleum*
 1433 *Geoscience*, 19(4), 329-341, 2013.
 1434
- 1435 Luth, S., Willingshofer, E., Sokoutis, D. and Cloetingh, S.: analogue modelling of
 1436 continental collision: Influence of plate coupling on mantle lithosphere subduction,
 1437 crustal deformation and surface topography, *Tectonophysics*, 4184, 87-102, doi:
 1438 10.1016/j.tecto2009.08.043, 2010.
- 1439 Maher, H. D., Jr., Bergh,S., Braathen, A. and Ohta, Y.: Svartfjella, Eidembukta, and
 1440 Daudmannsodden lineament: Tertiary orogen-parallel motion in the crystalline
 1441 hinterland of Spitsbergen's fold-thrust belt, *Tectonics*, 16(1), 88–106,
 1442 doi:10.1029/96TC02616, 1997.
- 1443 Mandl, G., de Jong, L.N.J. and Maltha, A.: Shear zones in granular material. *Rock*
 1444 *Mechanics*, 9, 95–144, 1977.
 1445
- 1446 Manduit, T. and Dauteuil, O.: Small scale modeling of oceanic transform zones,
 1447 *Journal of Geophysical Research*, 101(B9), 20195-20209, 1996.
 1448
- 1449 Mann, P.: Global catalogue, classification and tectonic origins o frestraining and

1450 releasing bends on active and ancient strike-slip fault systems. *in*: Cunningham, W.D.
 1451 and Mann, P. (eds.), 2007: Tectonics of Strike-Slip Restraining and Releasing Bends,
 1452 Geological Society London Special Publication, 290, 13-142, 2007.
 1453
 1454 Mann, P., Hempton, M.R., Bradley, D.C. and Burke, K.: Development of pull-apart
 1455 basins. *Journal of Geology*, 91(5), 529-554, 1983.
 1456
 1457 Mascle, J. & Blarez, E.: Evidence for transform margin evolution from the Ivory
 1458 Coast Ghana continental margin, *Nature*, 326, 378-381, 1987.
 1459
 1460 McClay, K.R., 1990: Extensional fault systems in sedimentary basins. A review of
 1461 analogue model studies, *Marine and Petroleum Geology*, 7, 206-233, 1990.
 1462
 1463 Mitra, S.: Geometry and kinematic evolution of inversion structures. *American*
 1464 *Association of Petroleum Geologists Bulletin*, 77, 1159-1191, 1993.
 1465
 1466 Mitra, S. and Paul, D.: Structural geology and evolution of releasing and
 1467 restraining bends: Insights from laser-scanned experimental models, *American*
 1468 *Association of Petroleum Geologists Bulletin*, 95(7), 1147-1180, 2011.
 1469
 1470 Morgenstern, N.R. and Tchalenko, J.S.: Microscopic structures in kaolin subjected to
 1471 direct shear, *Géotechnique*, 17, 309-328, 1967.
 1472
 1473 Mosar, J., Torsvik, T.H. & the BAT Team: Opening of the Norwegian and Greenland
 1474 Seas: Plate tectonics in mid Norway since the late Permian. in: E.Eide (ed.):
 1475 BATLAS. Mid Norwegian plate reconstruction atlas with global and Atlantic
 1476 perspectives. Geological Survey of Norway, 48-59, 2002.
 1477
 1478 Mouslopoulou, V., Nicol, A., Little, T.A. and Walsh, J.J.: Terminations of large-
 1479 strike-slip faults: an alternative model from New Zealand, in: Cunningham, W.D. and
 1480 Mann, P. (eds.): Tectonics of Strike-Slip Restraining and Releasing Bends,
 1481 Geological Society London Special Publication, 290, 387- 415, 2007.
 1482
 1483 Mouslopoulou, V., Nicol, A., Walsh, J.J., Beetham, D. and Stagpoole, V.: Quaternary
 1484 temporal stability of a regional strike-slip and rift fault interaction. *Journal of*
 1485 *Structural Geology*, 30, 451-463, 2008.
 1486
 1487 Myhre, A.M. and Eldholm, O.: The western Svalbard margin (74-80°N). *Marine and*
 1488 *Petroleum Geology*, 5, 134-156, 1988.
 1489
 1490 Myhre, A.M., Eldholm, O. and Sundvor, E.: The margin between Senja and
 1491 Spitsbergen Fracture Zones: Implications from plate tectonics. *Tectonophysics*, 89,
 1492 33-50, 1982.
 1493
 1494 Naylor, M.A., Mandl, G and Sijpestijn, C.H.K.: Fault geometries in basement-induced
 1495 wrench faulting under different initial stress states. *Journal of Structural Geology*, 8,
 1496 737-752, 1986.
 1497
 1498 Nemcok, M., Rybár, S., Sinha, S.T., Hermeston, S.A. and Ledvényioviá. L.:
 1499 Transform margins: development, controls and petroleum systems – an introduction.

1500 in: Nemcok, M., Rybár, S., Sinha, S.T., Hermeston, S.A. and Ledvényiová, L. (eds.):
 1501 Transform Margins,; Development, Control and Petroleum Systems, Geological
 1502 Society London, Special Publication, 431, 1-38, 2016.
 1503
 1504 Odonne, F. and Vialon, P.: Analogue models of folds above a wrench fault,
 1505 Tectonophysics, 990,31-46, 1983
 1506
 1507 Pace, P. and Calamita, F.: Push-up inversion structures v. fault-bend reactivation
 1508 anticlines along oblique thrust ramps: examples from the Apennines fold-and-thrust-
 1509 belt, Italy, Journal Geological Society London, 171, 227-238, 2014.
 1510
 1511 Pascal, C. and Gabrielsen, R.H.: Numerical modelling of Cenozoic stress patterns in
 1512 the mid Norwegian Margin and the northern North Sea. Tectonics, 20(4), 585-599,
 1513 2001.
 1514
 1515 Pascal, C., Roberts, D. and Gabrielsen, R.H.: Quantification of neotectonic stress
 1516 orientations and magnitudes from field observations in Finnmark, northern Norway.
 1517 Journal of Structural Geology, 27, 859-870, 2005.
 1518
 1519 Peacock, D.C.P., Nixon, C.W., Rotevatn, A., Sanderson, D.J. and Zuluaga, L.F.:
 1520 Glossary of fault and other fracture networks, Journal of Structural Geology, 92,
 1521 12-29, doi: 10.1016/j.jgs2016.09.008, 2016.
 1522
 1523 Perez-Garcia, C., Safranova, P.A., Mienert, J., Berndt, C. and Andreassen, K.:
 1524 Extensional rise and fall of a salt diapir in the Sørvestsnaget Basin, SW Barents Sea.
 1525 Marine and Petroleum Geology, 46, 129-134, 2013.
 1526
 1527 Planke, S., Alvestad, E. and Eldholm, O.: Seismic characteristics of
 1528 basaltic extrusive and intrusive rocks: The Leading Edge, 18(3), 342-348. [https://doi-](https://doi.org.ezproxy.uio.no/10.1190/1.1438289)
 1529 [org.ezproxy.uio.no/10.1190/1.1438289](https://doi.org.ezproxy.uio.no/10.1190/1.1438289), 1999.
 1530
 1531 Ramberg, H.: Gravity, deformation and the Earth's crust, Academic Press, New York,
 1532 214pp, 1967.
 1533
 1534 Ramberg, H.: Gravity, deformation and the Earth's crust, 2nd edition. Academic
 1535 Press, New York 452pp, 1981
 1536
 1537 Ramsay, J.G. and Huber, M.I., 1987: The techniques of modern structural geology.
 1538 Vol. 2: Folds and fractures. Academic Press, London, 309-700, 1987.
 1539
 1540 Reemst, P., Cloetingh, S. and Fanavoll,S.: Tectonostratigraphic modelling of
 1541 Cenozoic uplift and erosion in the south-western Barents Sea. Marine and Petroleum
 1542 Geology, 11, 478-490, 1994.
 1543
 1544 Richard, P.D., Ballard, B., Colletta, B and Cobbold, P.R.: Naissance et evolution de
 1545 failles au dessus d'un décrochement de socle: Modeléisation experimental et
 1546 tomographie, C. R. Acad.Sci. Paris, 308,9, 2111-2118, 1989.
 1547

1548 Richard, P.D. and Cobbold, P.R.: Structures et fleur positives et décrochements
1549 crustaux: modélisation analogique et interpretation mécanique, C.R.Acad.Sci.Paris,
1550 308, 553-560, 1989.

1551
1552 Richard, P. and Krantz, R.W.: Experiments on fault reactivation in strike-slip mode,
1553 Tectonophysics, 188, 117-131, 1991.

1554
1555 Richard, P., Mocquet, B. and Cobbold, P.R., 1991: Experiments on simultaneous
1556 faulting and folding above a basement wrench fault, Tectonophysics, 188, 133-141.
1557 1991.

1558
1559 Riedel, W.: Zur Mechanik geologischer Brucherscheinungen. Centralblatt für
1560 Mineralogie, Geologie und Paläontologie, 1929B, 354-368, 1929.

1561
1562 Riis, F., Vollset, J. & Sand, M.: Tectonic development of the western margin of the
1563 Barents Sea and adjacent areas. in: M.T.Halbouty (ed.): Future petroleum provinces
1564 of the World. American Association of Petroleum Geologists Memoir, 40, 661-667,
1565 1986.

1566
1567 Roberts, D.G., : Basin inversion in and around the British Isles, in: M.A.Cooper &
1568 G.D.Williams (eds.): Inversion Tectonics. Geological Society of London Special
1569 Publication, 44, 131-150, 1989.

1570
1571 Ryseth, A., Augustson, J.H., Charnock, M., Haugrud, O., Knutsen, S.-M., Midbøe,
1572 P.S., Opsal, J.G. and Sundsbø, G.: Cenozoic stratigraphy and evolution of the
1573 Sørvestsnaget Basin, southwestern Barents Sea. Norwegian Journal of Geology, 83,
1574 107-130, 2003.

1575
1576 Saunders, A.D., Fitton, J.G., Kerr, A.C., Norry, M.J., and Kent, R.W.: The North
1577 Atlantic Igneous Province: Geophysical Monograph 100, American Geophysical
Union, 45-93, 1997.

1578
1579 Scheurs, G.: Experiments on strike-slip faulting and block rotation, Geology, 22, 567-
1580 570, 1990.

1581
1582 Schreurs, G.: Fault development and interaction in distributed strike-slip shear zones:
1583 an experimental approach. in: Storti, F., Holdsworth, R.E. and Salvini, F. (eds):
1584 Intraplate Strike-slip Deformation Belts, Geological Society of London Special
1585 Publication, 210, 35-82., 2003.

1586
1587 Schreurs, G., and Colletta, B.. Analogue modelling of faulting in zones of
1588 continental transpression and transtension. in: Holdsworth, R.E., Strachan, R.A.,
1589 Dewey, J.F. (eds.), Continental Transpressional and Transtensional Tectonics,
1590 Geological Society of London Special Publication, London, 135, 59-79, 1998.

1591
1592 Schreurs, G. and Colletta, B.: Analogue modelling of continental transpression
1593 and transtension. in: Scellart, W.P. & Passchier, C. (eds.): Analogue Modelling of
1594 Large-scale Tectonic Processes. Journal of the Virtual Explorer, 7, 103-114,
1595 2003.

- 1596 Seiler, C., Fletcher, J.M., Quigley, M.C., Gleadow, A.J and Kohn, B.P.: Neogene
 1597 structural evolution of the Sierra San Felipe, Baja California: evidence of proto-gulf
 1598 transtension in the Gulf Extensional Province? *Tectonophysics*, 488(1), 87-109, 2010.
 1599
 1600 Sibuet, J.C. and Mascle, J.: Plate kinematic implications of Atlantic equatorial
 1601 fracture zone trends. *Journal of Geophysical Research*, 85, 3401-3421, 1978.
 1602 Sims, D., Ferrill, D.A. and Stamatakos, J.A.: Role of a brittle décollement in the
 1603 development of pull-apart basins: experimental results and natural examples. *Journal*
 1604 *of Structural Geology*, 21, 533-554, 1999.
 1605
 1606 Sokoutis D.: Finite strain effects in experimental mullions. *Journal of Structural*
 1607 *Geology*, 9, 233-249, 1987.
- 1608 Stearns, D.W., 1978: Faulting and forced folding in the Rocky Mountains
 1609 Foreland, *Geological Society of America Memoir*, 151, 1-38, 1978
 1610
 1611 Sylvester, A.G. (ed); 1985: Wrench Fault Tectonics, Selected papers reprinted from
 1612 the AAPG Bulletin and other geological journals, American Association of Petroleum
 1613 Geologists Reprint Series 28,3 74pp, 1985.
 1614
 1615 Sylvester, A.G.: Strike-slip faults. *Geological Society of America Bulletin*, 100, 1666-
 1616 1703, 1988.
 1617
 1618 Taylor, B., Goodlife, A. and Martinez, F.: Initiation of transform faults at rifted
 1619 continental margins, *Comptes Rendu Geosciences*, 341, 428-438, 2009.
 1620
 1621 Talwani, M. & Eldholm, O.: Evolution of the Norwegian-Greenland Sea. *Geological*
 1622 *Society of America Bulletin*, 88, 969-999, 1977.
 1623
 1624 Tchalenko, J.S: Similarities between shear zones of different magnitudes. *Geological*
 1625 *Society of America Bulletin*, 81, 1625-1640, 1970
- 1626 Tron, V. and Brun J-P.: Experiments on oblique rifting in brittle-ductile systems.
 1627 *Tectonophysics*, 188(1/2), 71-84, 1991.
- 1628 Twiss, R.J. and Moores, E.M.: *Structural Geology*, 2nd Edition, W.H. Freeman & Co.,
 1629 New York, -736pp, 2007.
 1630
 1631 Ueta, K., Tani, K. and Kato, T.: Computerized X-ray tomography analysis of three-
 1632 dimensional fault geometries in basement-induced wrench faulting, *Engineering*
 1633 *Geology*, 56, 197-210, 2000
 1634
 1635 Uliana, M.A., Arteaga, M.E., Legarreta, L., Cerdan, J.J. and Peroni, G.O.: Inversion
 1636 structures and hydrocarbon occurrence in Argentina. *in*: Buchanan, J.G. &
 1637 Buchanan, P.G. (eds.): *Basin Inversion*, Geological Society London Special
 1638 Publication, 88, 211-233, 1995
 1639
 1640 Vågnes, E., 1997: Uplift at thermo-mechanically coupled ocean-continent transforms:
 1641 modeled at the Senja Fracture Zone, southwestern Barents Sea. *Geo-Marine Letters*,
 1642 17, 100-109, 1997.

1643 Vågnes, E., Gabrielsen, R.H. and Haremo. P.: Late Cretaceous-Cenozoic intraplate
1644 contractional deformation at the Norwegian continental shelf: timing, magnitude and
1645 regional implications. *Tectonophysics*, 300, 29-46, 1998.

1646 Weijermars, R. and Schmeling, H.: Scaling of Newtonian and non-Newtonian
1647 fluid dynamics without inertia for quantitative modelling of rock flow due to
1648 gravity (including the concept of rheological similarity. *Physics of the Earth and*
1649 *Planetary Interiors*, 43, 316-330, 1986.

1650 Wilcox, R.E., Harding, T.P. and Selly,D.R.: Basic wrench tectonics. *American*
1651 *Association of Petroleum Geologists Bulletin*, 57, 74-69, 1973

1652
1653 Williams, G.D., Powell, C.M., and Cooper, M.A.: Geometry and kinematics of
1654 inversion tectonics. in: M.A.Cooper & G.D.Williams (eds.): *Inversion Tectonics*.
1655 *Geological Society of London Special Publication*, 44, 3-16, 1989.

1656
1657 Willingshofer, E., Sokoutis, D. and Burg, J.-P.: Lithosphere-scale analogue modelling of
1658 collision zones with a pre-existing weak zone, *in: Gapais,D., Brun.,J.P.& Cobbold,P.R.*
1659 *(eds.): DeformationMechanisms, Rhology and Tectonics: from Minerals to the*
1660 *Lithosphere*, *Geological Society London Special Publication*,43, 277-294, 2005.

1661
1662 Willingshofer, E., Sokoutis, D., Beekman ,F. Schönebeck, F., Warsitzka, J.-M., Michael,
1663 M. and Rosenau, M.: Ring shear test data of feldspar sand and quartz sand used in
1664 the Tectonic Laboratory (TecLab) at Utrecht University for experimental Earth
1665 Science applications. V. 1. GFZ Data Service.
1666 <https://doi.org/10.5880/idgeo.2018.072>, 2018.

1667
1668 Woodcock, N.H. and Fisher, M.,1986: Strike-slip duplexes. *Journal of Structural*
1669 *Geology*, 8(7), 725-735, 1986.

1670
1671 Woodcock, N.H. and Schubert, C.: Continental strike-slip tectonics. in: P.L.Hancock
1672 (ed.): *Continental Deformation* (Pergamon Press), 251-263, 1994.

1673
1674 Yamada, Y. and McClay, K.R.: Analog modeling of inversion thrust structures,
1675 experiments of 3D inversion structures above listric fault systems, in: McClay,K.R.
1676 (ed.): *Thrust Tectonics and Petroleum Systems*, *American Association of Petroleum*
1677 *Geologists Memoir*, 82, 276-302, 2004.

1678
1679
1680
1681
1682
1683
1684
1685
1686

1687
1688
1689
1690